Investigating the Interaction of Biomolecular Systems with Graphene-like Materials

Submitted in partial fulfilment of the requirements for the degree of Master of Technology

By

Sankhadip Saha

Roll No. 193110065

Under the guidance of

Prof. Sumit Saxena

Department of Metallurgical Engineering and Materials Science

INDIAN INSTITUTE OF TECHNOLOGY BOMBAY

2021

Dissertation Approval Sheet

The dissertation entitled "**Investigating the Interaction of Biomolecular Systems with Graphene-like Materials**" submitted by **Sankhadip Saha** (Roll No:193110065) is approved for the degree of Master of Technology in Metallurgical Engineering and Material Science (Specialization: Corrosion Science and Engineering) from Indian Institute of Technology, Bombay.

Date: 24th June 2021

Project Guide

Chairman

Co-Guide

External Examiner

Internal Examiner

Declaration

I hereby declare that this written submission is the presentation of my ideas in my own words and where other's ideas or words have been included. I have adequately cited and referenced the original source. I also declare that I have adhered to all principles of academic honesty and integrity and haven't misrepresented or fabricated or falsified any data/idea/fact source in my submission. I understand that any infringement of the above will be cause for disciplinary action by the Institute and can invoke penal action from the sources which have thus not been properly cited or from whom the proper permission has not been taken wherever required.

(Signature)

Sankhadip Saha

193110065

Acknowledgement

I would like to take this opportunity to express a deep sense of gratitude to my guide, Prof. Sumit Saxena and my mentor, Dr. Basant Roondhe for imparting their knowledge and for teaching me the art of research. Their continuous encouragement and competent guidance motivated me and instilled a sense of confidence in me. I also thank all other professors of Metallurgical Engineering and Material Science Department, Indian Institute of Technology, Bombay who have given their invaluable time in sharing their thoughts on various subjects.

I am also grateful to my friend, Ms. Megha, for her valuable time in helping me out in various stages of my project.

Finally, I must mention the relentless support and endless sacrifices by my parents for which I shall be forever obliged.

Sankhadip Saha

IIT Bombay,

24th June 2021

ABSTRACT

sp^2-hybridized carbon atoms arranged in planar sheet and tightly packed in 2D honeycomb lattice, gives rise to one of those talismans for present day material scientists: Graphene. It's widespread popularity as a wonder material lies deep in graphene's distinctive electronic structure that bestows it with high electron mobility and in its ability to interact with molecules. Significant doping strategies have also been explored to modify the intrinsic properties of graphene. Among the diverse domain of graphene, bio-conjugated graphene nanostructures in drug delivery and medical diagnostics have sparked significant interest. Graphene's ability to pass through biological membranes provided considerable motivation to investigate its interactions with different biomolecules such as nucleobases and amino acids. Among Amino Acids (AAs), particularly in the set of essential AAs, Branched-Chain AAs (BCAAs) have been linked with number of disorders, particularly in liver cirrhosis, renal failure and insulin resistance. Specifically, high plasma valine concentration is associated with Type-2 Diabetes whereas increased extracellular concentration of valine improves dendritic cell function in cirrhosis patients. Stated its biological significance, evaluation of valine/modified-graphene bioconjugate systems might unlock potential pathways for future diagnosis. Our present study would be instrumental in technical recognition of graphene in the targeted delivery of valine, revealing the underlying physics and chemistry behind graphene-biomolecules interactions at molecular level to foster it's biomedical application. In this work, we performed first principle calculations within the framework of Density Functional Theory to understand the adsorption behaviour of Valine on Silicon doped Graphene surface . The calculated structural and electronic properties provided the base for explaining the adsorption study. Si-doped Graphene was found to have better adsorption energy for valine with respect to Pristine Graphene. In order to investigate it's biosensing capability, recovery time calculations were also performed which showed ultrafast recovery time of 92ms for Valine. The findings of this work suggests that Silicon doped Graphene can be used as a biosensor for Valine owing to it's enhanced properties with respect to graphene.

Table of Contents

List of Figures.....3
List of Tables.....4
CHAPTER: 1 Introduction.....5
1.1 Background and Motivation.....5
CHAPTER: 2 Literature Review.....6
2.1 2-D Materials.....6
2.2. Graphene: The Wonder Material.....6
2.2.1. Brief history of Graphene.....7
2.2.2. Properties and Applications of Graphene.....10
2.3. Modified Graphene and It's Applications.....13
2.4. Computational Study of Graphene.....14
2.5. Bio-conjugate Systems……...16
2.6. Amino Acids……..19
2.6.1 Valine Amino Acids.....22
CHAPTER: 3 Aim of Present Work.....25
3.1 Choice of Dopant Atom ……..26
CHAPTER: 4 Density Functional Theory.....27
4.1 Origin.....27
4.1.1 Many Body Problem ……27
4.2 Wave Function Based Method To Solve Many Body Problem..... ……29
4.2.1 Born Oppenheimer Approximation…….……..29
4.2.2 Hartree Approximation…...…….…….……29
4.2.3 Hartree Fock Approximation…….……..…….30

4.3 Density Functional Theory: Density based Method…….....31

4.3.1 Thomas-Fermi Theory…….. ……31

4.3.2 Hohenberg and Kohn Theory..……...32

4.3.3 Kohn-Sham Equation……...,…….34

4.3.4 Self-Consistency in K-S Equation……36

4.4 Exchange and Correlation Functional……..37

4.4.1 Local Density Approximation(LDA)……38

4.4.2 Generalized Gradient Approximation(GGA)……38

4.4.3 Pseudopotentials……...39

4.5 Dispersion Correction in Density Functional Theory…….40

CHAPTER: 5 Interaction of Valine with Modified Graphene: A Dispersion Corrected Density Functional Theory Study……41

5.1 Computational Methods……...……..41

5.2 Results and Discussion……..……45

5.2.1 Structural Properties...……..……..45

5.2.2 Electronic Properties……..……50

5.2.3 Adsorption……..……...54

5.2.4 Recovery Time……..……60

CHAPTER: 6 Summary and Future Work……..……62

References…….……...63

List of Figures

Figure 2.1 : Single layer graphene was first observed by Geim et. al. Here a few layer flake is shown.[2]…….7
Figure 2.2 : Diagram showing the process of Intercalation and Exfoliation. Here Potassium is introduced between the layers and reacted violently.[2]……8
Figure 2.3 : SEM images showing a) before and b) after the expansion of Graphite Layers by Acid Intercalation.[2]…….. 9
Figure 2.4: a) AFM image of Graphene; b) TEM image of free standing Graphene film.[2]……9
Figure 2.5 : 2-D Hexagonal sheet of carbon atoms : Graphene sheet[12]…….10
Figure 2.6: Stacking Sequence of Graphene[12]……..11
Figure 2.7: Band Structure of Single layer Graphene[11]……11
Figure 2.8 : p- and n-type doping.[26]……...13
Figure 2.9a) Heteroatom doping in Graphene.[26]……13
Figure 2.9b) Doping by adsorption.[27]……13
Figure 2.10 : L-Leucine interacting with Graphene surface in four different arrangements[34]…….….16
Figure 2.11 : Optimized geometries of a) Graphene and b) BN [64]……..18
Figure 2.12: Optimized structures of a) Pristine Graphene, b) Graphitic N, c) Pyridinic 1N and d) Pyridinic 3N [68]……..21
Figure 2.13: Optimized structures of a) Graphdiyne(GD), b) Pristine Graphene(GP).[69]…….22
Figure 2.14 : Chemical structure of Valine. [64]……..22
Figure 2.15 : Optimized geometries of Valine on Graphene, BN sheets and Dispersion corrected geometries for BN sheet(left to right) [64]……..23
Figure 3.1 : Schematic of biosensing application…….25
Figure 4.1: The flowchart of Self Consistency calculation.[source: DFT Tutorial]……36
Figure 5.1 : Flow diagram of Unit Cell Optimization……..41
Figure 5.2 : Final Energy Vs Energy Cutoff value……...42
Figure 5.3 : Final Energy Vs Number of K-points……...42
Figure 5.4 : Final Energy Vs Lattice Parameter…… 43
Figure 5.5 : Flow Chart for calculations of the sheet……....43
Figure 5.6 : Schematic of the unit cell, graphene and doped graphene sheet……..… 44
Figure 5.7 : The optimized structure of Pristine Graphene sheet…….. ...…45
Figure 5.8: The optimized structure of Si-doped Graphene sheet……..… .46
Figure 5.9: The bond angles in the Hexagonal rings around the doping site in Pristine Graphene……..…....47
Figure 5.10: The bond angle changes in the Hexagonal rings around the doping site in Si-doped Graphene……..48
Figure 5.11: The optimized structure of Valine molecule in different orientations……....49
Figure 5.12: The doping site atom(C^*) and the adjacent atom(C) depicted on the graphene sheet……50
Figure 5.13: The band structure, DOS and PDOS of Pristine Graphene……51
Figure 5.14: The band structure, DOS and PDOS of Si-doped Graphene……..……...51
Figure 5.15: Partial DOS of Pristine Graphene……...52

Figure 5.16: Partial DOS of Si-doped Graphene……53
Figure 5.17: The optimized structure of Valine adsorbed on Pristine Graphene……...54
Figure 5.18: The optimized structure of Valine adsorbed on Si-doped Graphene…….55
Figure 5.19 : The distance between the molecule and Pristine Graphene sheet……55
Figure 5.20: The distance between the molecule Si-doped Graphene sheet……..56
Figure 5.21 : Band Structure, DOS and PDOS of Pristine Graphene + Valine combined system…….57
Figure 5.22 : Partial DOS of Valine adsorption on Pristine Graphene showing the effective contribution of the orbitals to the DOS……..58
Figure 5.23: Band Structure, DOS and PDOS of Si-doped Graphene + Valine combined system.....59
Figure 5.24: Band Structure, DOS and PDOS of Si-doped Graphene + Valine combined system.....59
Figure 5.25: Recovery Time of Valine adsorbed on a) Pristine Graphene and b) Si-doped Graphene with increase in Temperature……...61

List of Tables

Table 2.1 BCAA and their Immune function[66].....20
Table 2.2 Adsorption energy (ΔE_{ad}) values of valine adsorbed on nano-surfaces in gaseous and solvent phases.[64]……...24
Table 5.1 Bond length and Bond angle of the optimized systems……...47
Table 5.2 Lattice parameters, D, E_g and E_F of the optimized systems…….49

CHAPTER 1 : Introduction

1.1 Background and Motivation

With the first successful synthesis of Single Layer Graphene by the method of mechanical exfoliation, a considerable focus has been on utilizing it's properties for solving various problems. From being used in sensors to air filters Graphene has been the go-to material of the 21st century. Given it's high surface area, biocompatibility, adjustable layer numbers and dimension and surface chemistry, they have enabled their usage in biomedical research. Therefore, due to this increase in synthesis of Graphene for biomedical purposes, it is very important to understand the fundamental interaction mechanisms of Graphene with the biomolecules.

Extensive literature review showed that a considerable amount of work has been done in order to understand the interaction mechanisms between amino acids, nucleobases and other organic biomolecules. Also, in order to overcome the intrinsic limitations of Pristine Graphene, various modified Graphene have been studied. Amino acids are the building blocks for protein and thus, in order to have an indepth knowledge of protein mechanisms, it is of utmost importance to know the amino acids in details. For instance, the way amino acids interact with various inorganic materials, provides an insight into their behaviour with biological implants.

Valine which is an essential Amino Acid, is important for biological processes of the body and deficiency of it may lead to various ailments. For instance, high plasma valine concentration is associated with Type-2 Diabetes whereas increased extracellular concentration of valine improves dendritic cell function in cirrhosis patients. Therefore, it will be fruitful if we could understand the mechanism of interaction of Valine with Graphene/Modified Graphene resulting in new Bio-conjugate systems.

In the Literature available, theoretical works on interaction mechanisms have only been limited to Pristine Graphene, BN sheets and N-doped Graphene. Thus, having known the importance of understanding such interactions, we venture into theoretical study of Valine interactions with Graphene and Modified Graphene.

CHAPTER 2 : Literature Review

2.1 Two-Dimensional (2-D) Materials

The 2-D materials field sprouted with the successful synthesis of Graphene by Novoselov, Geim, and co-workers. Graphene was synthesized by the process of mechanical exfoliation using Scotch tape from Graphite Flakes. This very event opened the gates to explore a very interesting group of materials that are single atom thick with varying length and breadth. In the successive decade-and-a-half the scientific community has shown great enthusiasm to venture into the fascinating world of these materials, thus taking the scope of these materials from graphene and beyond. Significant amount of interest have also been focused on graphene-analogous 2D materials, including the transition metal dichalcogenides (TMDs), graphitic carbon nitride (g-C3N4), hexagonal boron nitride (h-BN), black phosphorus (BP), MXenes, silicene, etc. Their unique physical, electronic, optical, and chemical properties as well as the scope of new applications arising from these properties have captivated researchers from diverse fields such as condensed matter physics, materials science, chemistry, and nanotechnology. For example, the electron confinement in 2D materials offer intriguing electronic properties, which has stimulated the evolution of next generation electronic devices. Furthermore, their high specific surface area motivates their use in surface-sensitive applications, such as adsorption, catalysis and sensing. The atomic thickness and high anisotropy of 2-D materials bestows them with exceptional mechanical flexibility and optical transparency, which is advantageous in development of 2D material-based opto-electronic devices and wearable devices.[1]

Thus, the scientific *bees* continue to swill on the *Graphinic*-pot of nectar to brew the honey of innovations befitting the challenges of this world.

2.2 Graphene : The Wonder Material

Graphene is the name given to sp^2-hybridized carbon atoms arranged in planar sheet and tightly packed in 2D honeycomb lattice. It's extended network is the basic building block of other important allotropes; it can be stacked up to form 3-D graphite, rolled to form 1D nanotubes, and wrapped to form 0D fullerenes. Owing to it's long-range π-conjugation, graphene shows extraordinary thermal,

mechanical, and electrical properties which have long attracted the attention of many theoretical studies and recently became an exciting area for experimentalists.[2]

2.2.1 Brief History of Graphene

To understand the course of graphene research, it would be convenient to consider graphene simply as the fewest layer limit of graphite. Owing to it's layered morphology and weak dispersion forces between adjacent sheets, Graphite had been utilized in making marking instruments in the medieval ages , in a way similar it is used in pencils today. Recently, the same properties have made graphite an ideal material for use as a dry lubricant, along with the homologous but more expensive compounds h-BN and molybdenum disulfide. High in-plane thermal (~3000 W/mK) and electrical conductivity (~104 Ω-1 cm-1) has enabled the utilization of graphite in electrodes and as heating elements for industrial blast furnaces.[2]

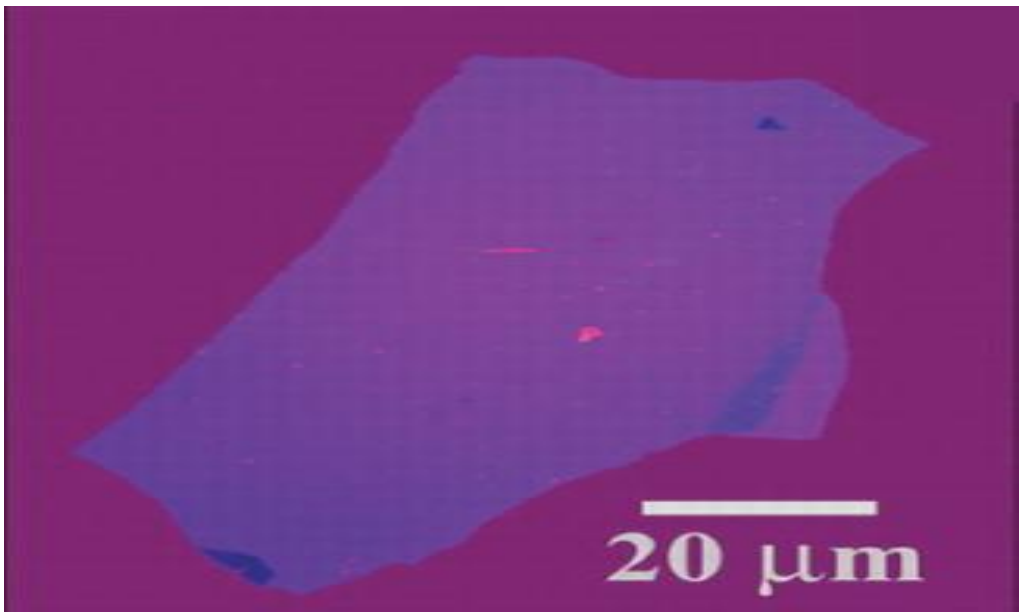

Fig.2.1 : Single layer graphene was first observed by Geim et. al. Here a few layer flake is shown.[2]

Graphite owing to it's rich chemistry can participate in reactions as either a reducing agent (electron donor) or an oxidizer (electron acceptor). This is a due to its electronic structure, which results in both an electron affinity and an ionization potential of 4.6 eV.[3] A large number of experiments have focussed on the insertion of additional chemical species between the basal planes of graphite, or intercalation. Shaffault et al. is credited with the first intercalation using potassium, in 1841.[4] Graphite intercalation compounds (GICs) appear to be the only layered compounds sufficiently ordered to show "staging" in which the number of layers in between adjacent intercalants can be

adjusted in a controlled fashion. Stage of a compound refers to the number of graphitic layers in between adjacent planes of the intercalant. Increased interlayer spacing in GICs means a significant reduction in the van der Waals forces between adjacent sheets pointing out their exfoliation as a possible route to single layers of graphene. Enoki et al. violently reacted a stage-1 potassium intercalation compound (KC8) with different solvents such as alcohols, but exfoliation produced only metastable slabs approximately 30 layers thick that had a tendency to scroll under high-powered sonication (see Figure 2.2).[3,5,6]

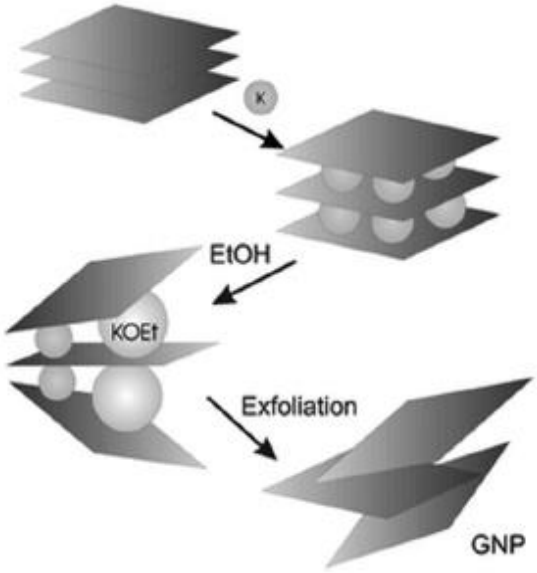

Fig.2.2 : Diagram showing the process of intercalation and exfoliation. Here, potassium is introduced between the layers and reacted violently.[2]

The spacing in GICs can be further increased by thermal shock to produce "expanded" graphite, which now serves as a starting material for recent techniques, including a nanoribbon synthesis developed by Dai (see Figure 2.3).[3,7] A second focus of experiments on graphite has been on substitutional doping, replacing carbon with other elements. Bartlett et al. substituted carbon with boron and nitrogen to form p-type and n-type graphite.[2]

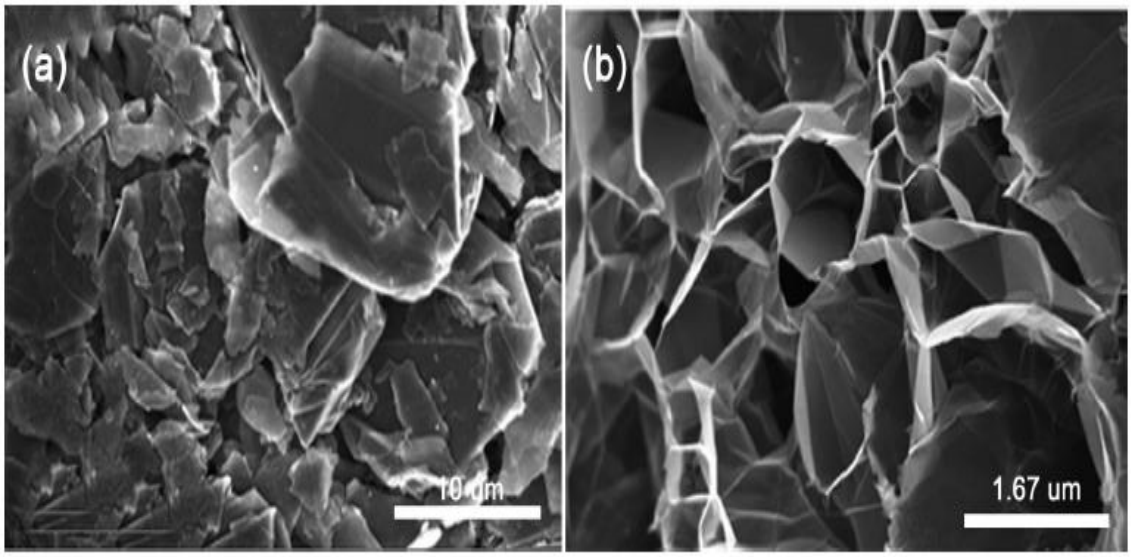

Fig.2.3 : SEM images showing a) before and b) after the expansion of graphite layers by acid intercalation.[2]

Researchers have tried to produce thinner samples by using the mechanical exfoliation of layers. Ruoff's group, in 1999, reported one such approach by using atomic force microscope (AFM) tip to manipulate small pillars patterned into highly oriented pyrolytic graphite (HOPG) by plasma etching.[8] At that time, the thinnest slabs observed were more than 200 nm thick. Kim et al. later refined the method by transferring the pillars to a tipless cantilever, which successively stamped down slabs as thin as 10 nm on SiO_2.[10] While these elegant methods produced thin samples, it was ultimately by employing a much simpler method, that Novoselov, Geim, and co-workers were able to isolate single layer graphene in 2004 group led by Geim (see Figures 2.4).[9]

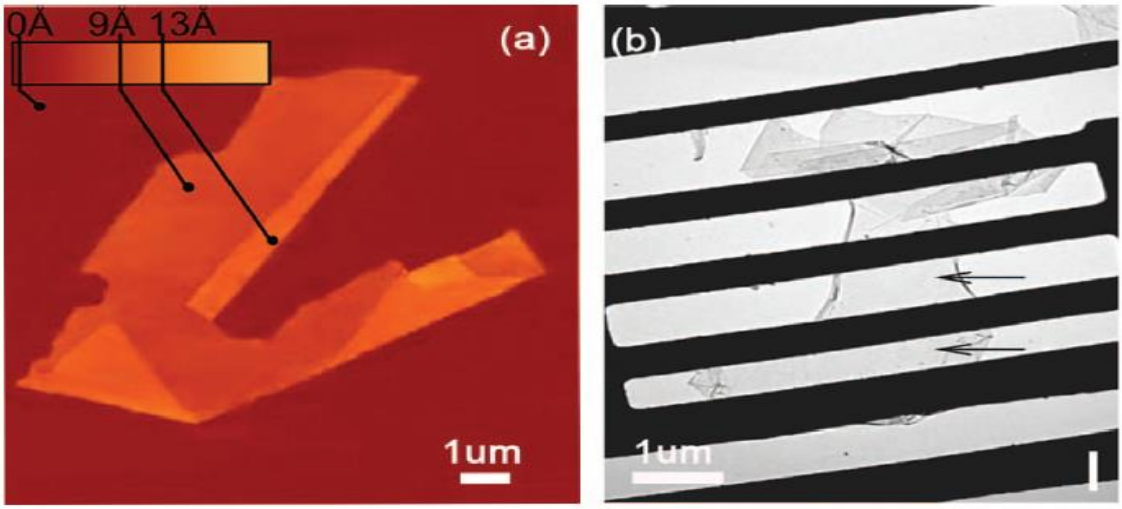

Fig.2.4: a) AFM image of Graphene; b) TEM image of free standing graphene film.[2]

The “peeling” method utilizes common cellophane tape to successively remove layers from a graphite flake. The tape is then pressed down against a substrate to deposit a sample. Although the flakes present on the tape are much thicker, van der Waals force to the substrate can delaminate a single sheet when the tape is lifted away.

2.2.2 Properties and Applications of Graphene

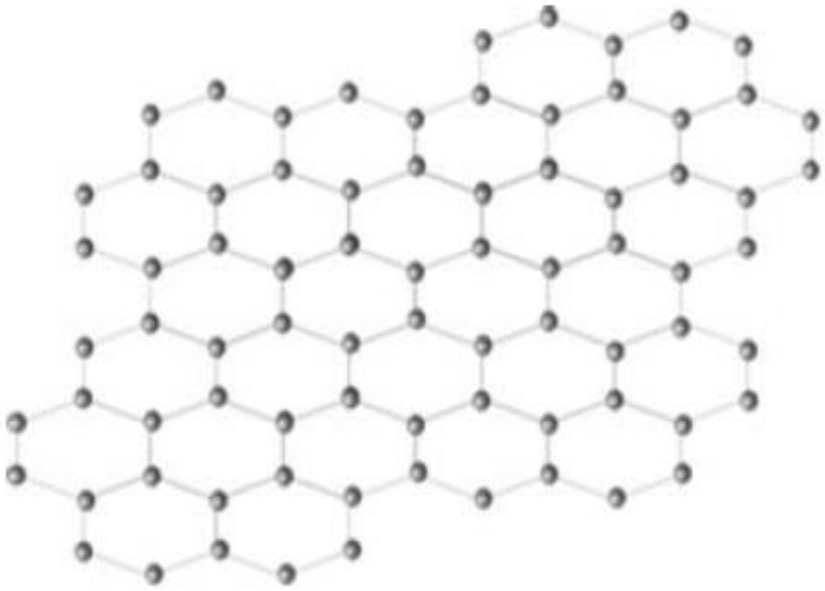

Fig. 2.5 : 2-D hexagonal sheet of carbon atoms : graphene sheet.[12]

With the successful synthesis of graphene, adequate interest developed in using it’s properties for various applications. A single-layer graphene is defined as a single 2-D hexagonal sheet of carbon atoms (Figure 2.5).[12] Bi-layer and few-layer graphene have 2 and 3 to 10 layers of such two-dimensional sheets, respectively. Graphene structures comprising of more than 10 such layers are categorized as thick graphene sheet and are of less scientific interest. C atoms in bi-layer and few-layer Graphene can be stacked in different ways namely hexagonal or AA stacking, Bernal or AB stacking and rhombohedral or ABC stacking (Figure 2.6). Graphene is sp^2 hybridized showing three in-plane σ bonds/atom and π orbitals perpendicular to the plane. While the strong σ bonds form the rigid backbone of the hexagonal structure, the out-of-plane π bonds controls the interaction between different graphene layers.[11]

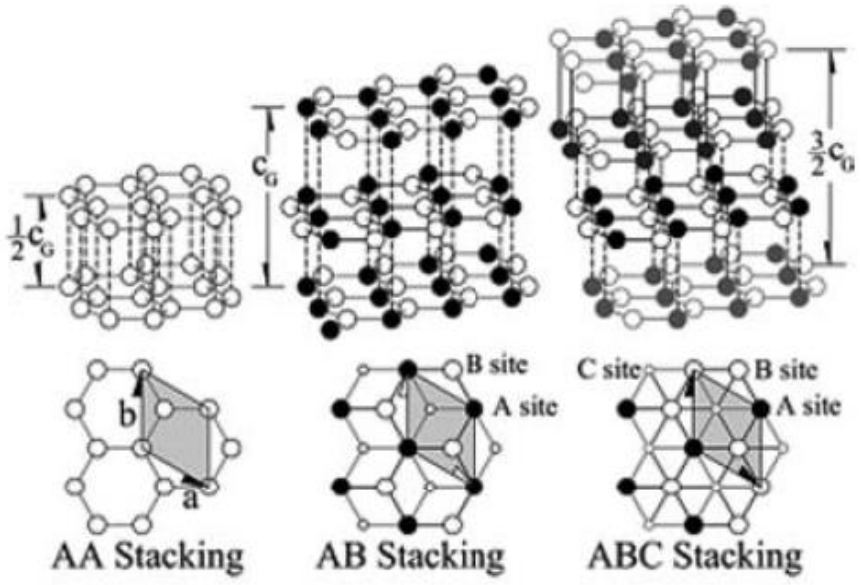

Fig. 2.6: Stacking sequence of graphene.[12]

The band-overlap in two conical points (K and K´) in the Brillouin zone (Figure 2.7) of Single-layer graphene(SLG) puts forth an unique electronic structure . The charge carriers, known as mass-less Dirac fermions, are electrons losing their rest mass (m_0) .[12-14] Therefore, SLG is expected to show some unusual properties in comparison with metals and semiconductors and typical of a semi-metal. Room-temperature ambipolar characteristics, i.e., the charge carriers can be alternated between holes and electrons depending upon the nature of the gate voltage, is also shown by SLG.

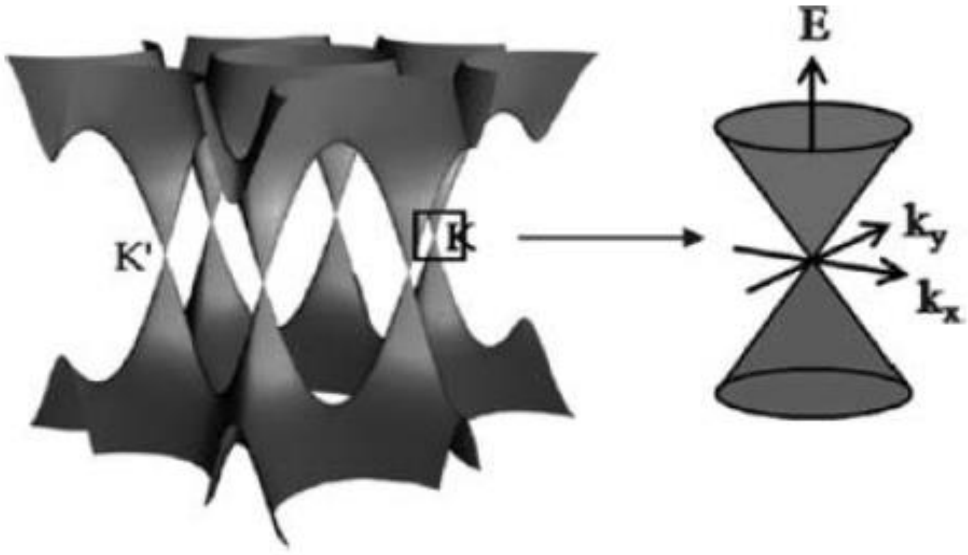

Fig. 2.7: Band structure of single layer graphene.[11]

Anomalous quantum Hall effect (QHE), at low temperature and room temperature has also been reported for SLG.[15-16] These unique properties of SLG have made it suitable for applications in

electronics and for studying basic quantum physics phenomena. Another important application of SLG is in gas sensing as the adsorbed gas molecules modify the local carrier concentration and cause subsequent change in the resistance. Schedin et. al. [17] prepared micron-level gas sensors, which can detect adsorption and desorption of single molecules of gases like CO, H_2O, NH_3 and NO_2. As graphene is electronically a very good low-noise material, molecular sensing could be achieved with this material.[18] Single-layer graphene is also attributed as one of the strongest materials. Strength of a defect-free, mono-layer graphene measured using nano-indentation technique and by atomistic simulation, both showed a Young's modulus of ∼1.0 TPa. [19]

Bio-compatible Graphene papers were prepared by Chen et al. using mechanically strong graphene sheets.[20] With such exciting new properties, graphene is expected to open up new areas of application. Gapless state with parabolic bands touching at K and K′ shown by Bi-layer Graphene , in contrast to conical bands of single-layer graphene, makes it a gapless semiconductor. Charge carriers in Bi-layer graphene, in contrast to SLG, have finite mass and called massive Dirac fermions. It also shows an anomalous QHE, but different from that of single-layer graphene and thus remains metallic at the neutrality points.[21] However, the carrier concentration changes with an application of gate voltage, therefore introducing asymmetry between the two layers. As a result the formation of a semiconducting gap takes place restoring the normal QHE.[22] However, Zhou and group have shown that an energy band gap of ∼0.26 eV is generated in graphene, when it is epitaxially grown on SiC substrate.[23] This makes graphene more suitable for application in electronics industries. Various Scientific Literatures have reported that the band gap decreases with increasing number of layers and approaches zero, as the structure has more than four layers. This band gap opening was proposed to be caused by graphene-substrate interaction and breaking of sublattice symmetry. In a related study, it was reported that graphene, epitaxially grown on C-terminated surface of 4H-SiC, have different stacking sequence.[24] Therefore, the structure, irrespective of the number of layers (up to ∼10 layers thick), shows an electronic structure similar to that of single-layer graphene and behaves like SLG. Furthermore, single- and bi-layer graphene shows very high transparency for light waves in the range of ultra-violet to infra-red, making it suitable for applications in solar cells.

Graphene due to its unique properties : high surface area, adjustable layer number, lateral dimensions and enhanced surface chemistry have wild areas Biomedical applications. Discussion on Graphene's application in Biological systems is mentioned in Section 2.5.

2.3 Modified Graphene and It's Applications

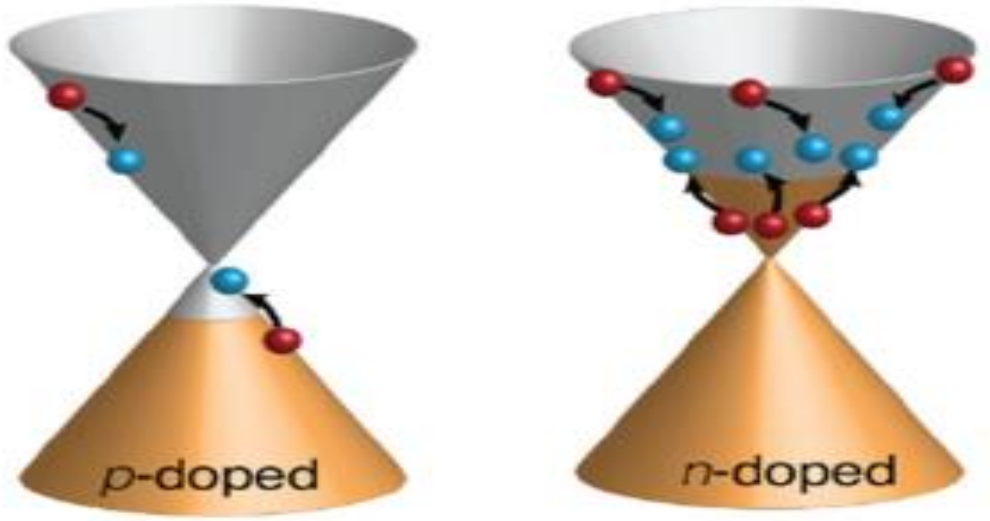

Fig. 2.8 : p- and n-type doping.[26]

The absence of semiconducting gap in pristine graphene have staggered the use of Graphene in electronic devices. Thus, considerable amount of research is focused on opening a sizeable and well-tuned bandgap for application in graphene-based electron-devices. Generally, two approaches have been employed: i) replacement or substitution of carbon atoms with heteroatoms and ii) incorporation of dopants through physical or chemical adsorption on the graphene surface. Substitution with heteroatom is inherently stable owing to the covalent bond linkage of the dopant in the base graphene lattice.[25]

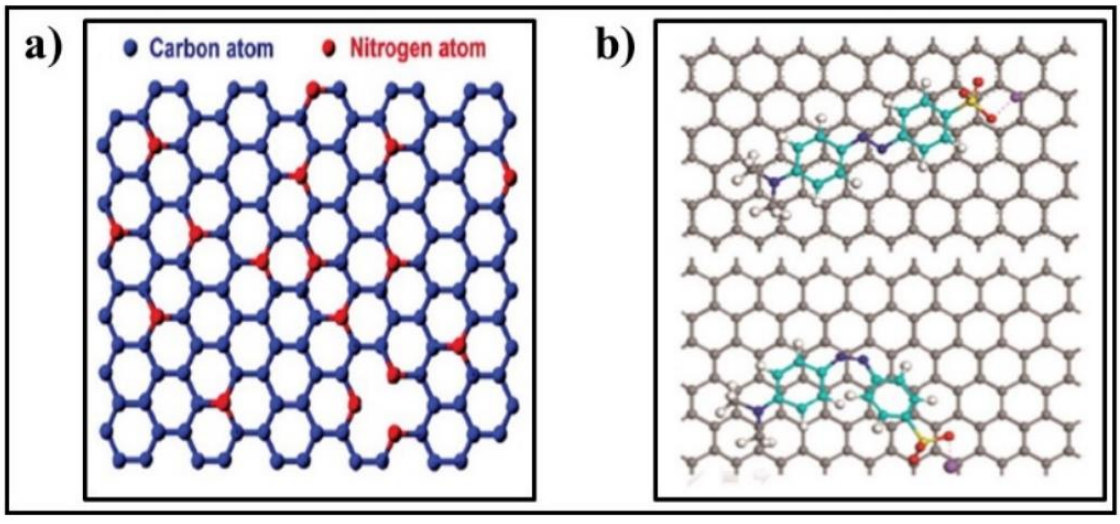

Fig. 2.9: a) Heteroatom doping in graphene[26] and b) Doping by adsorption.[27]

However, it disrupts graphene's unique honeycomb structure, inducing defects and disorder (Fig.2. 9a) [26], inducing a decrease of electronic mobility and hence degrading the performance of electrical devices. On the other hand, adsorption of electronically interacting dopants with graphene leads to local perturbation of graphene, resulting in desired doping (Fig. 2.9b) [27-28]. Though the structural integrity of the lattice is expected to be preserved; however, it doesn't guarantee a stable doping system. Furthermore, it should be important to understand how wide the range of hole or electron concentration can be controlled with the methods. Substitutional doping is an useful method to open bandgap of graphene. Various groups reported the B- and N-doping of graphene in the process of graphene synthesis. Boron and nitrogen have attracted significant attention as their atomic radii are similar to that of carbon. Nitrogen being the first dopant introduced in graphene, has been widely exploited for inducing n-type conductivity, thus representing a key element for the development of microelectronic devices. Zhang et al.[29] reported the N-doped graphene synthesis using the embedded C and N by CVD method. Temperature dependent electrical transport measurement showed that resistance of N-doped graphene decreased by more than 80-fold with the temperature increased from liquid nitrogen temperature to 300 K, thus showing semiconducting property of N-doped graphene. The bandgap (E_g) estimated was about 0.16 eV. From the electronic point of view, boron, unlike nitrogen, is less electronegative (even less than carbon), and induces p-type conductivity in graphene. Therefore, in order to further enhance and overcome the challenges in Pristine Graphene, various modified Graphene viz. doped Graphene with N-, B-, Si-,P- etc. have been studied. The tailored properties of these modifications have found applications in opto-electronics, electronic devices, photocatalysis and biomedical applications.

Since the base of all these experimental synthesis is rooted in the theoretical study of Graphene involving First Principle Techniques, therefore it will be interesting to venture into this genre of Material Science and get a taste of Computational Materials Research.

2.4 Computational Study of Graphene

Computational materials science includes computational tools for solving the challenges of materials related problems. Different mathematical models for investigating problems at multiple time and length scales which are instrumental in understanding the evolution of material structures (at different length scales) and how these structures effectively control various material properties. With this theoretical understanding we can select materials for specific applications and design relevant

advanced materials for new applications. Molecular Dynamics (MD) and Monte Carlo (MC) methods are considered as preferred tools for atomistic simulations whereas Density Functional Theory (DFT) is considered a popular computational tool.

Similarly a lot of theoretical calculation involving first principle techniques have been utilized to understand various interaction mechanism of Graphene along with extensive study to further enhance the system. It is interesting to know that long before the isolation of the Graphene from Graphite Flakes, theoretical studies have been conducted on the system unfolding it's various unique properties. Studies in order to understand the doping mechanism: how it actually works, the effect on the properties and subsequent areas of applications were reported.

First-principles calculations were carried out by Hussian and group to investigate the structural and electronic properties of beryllium (Be) and nitrogen (N) co-doped and BeN/BeO molecular doped graphene systems. They reported that the Fermi level rises or lowers depending upon the doped concentration of holes or electron. Doping of a hole (1Be) and electron (1N) produces a small energy gap of 0.30 eV. With Be and N are substituted on the same hexagon, the gap opening increased. Impurity substitution at different sub-lattice positions enhance the bandgap to 0.62 eV.[31]

Graphene-based materials for energy conversion and storage applications, Dobrota et al. performed a DFT study of Na interaction with doped graphene considering non-oxidized and oxidized forms. As the dopant atoms and vacancies act as OH groups attractors, it is of utmost importance to include them in the consideration. They reported that the type of the interaction of a given graphene based material with Na is highly dependent on its oxidation level.[32]

Considerable focus have been implied on studying the mechanism and adsorption affinity of various molecules on pristine graphene as well as on doped/modified graphene. Adsorption study of O_3, SO_2 and SO_3 molecules on the surface of a B-doped graphene conducted by Rad et al. showed weak physisorption for SO_2 (10.9 kJ/mole) and SO_3 (15.7 kJ/mole) whereas strong chemisorption was reported for O_3 (96.3 kJ/mole). Thus, suggesting that B-doped graphene as a potential adsorbent for O_3 molecule.[33]

The unique properties of graphene have found suitable applications in the field of biomedical research providing effective solutions to the most challenging problems. For example, a study has shown that superparamagnetic graphene oxide-Fe3O4 hybrid can be loaded with anti-cancer drug doxorubicin hydrochloride[36], and fluorescein-based dye-labeled graphene oxide has been reported to be a

sensitive and selective platform for target protein detection, without the interfering with other proteins [35]. Alwarappan et. al. have found that graphene electrodes exhibited better biosensing performance with respect to CNTs toward dopamine detection in the presence of interfering agents such as ascorbic acid[37].

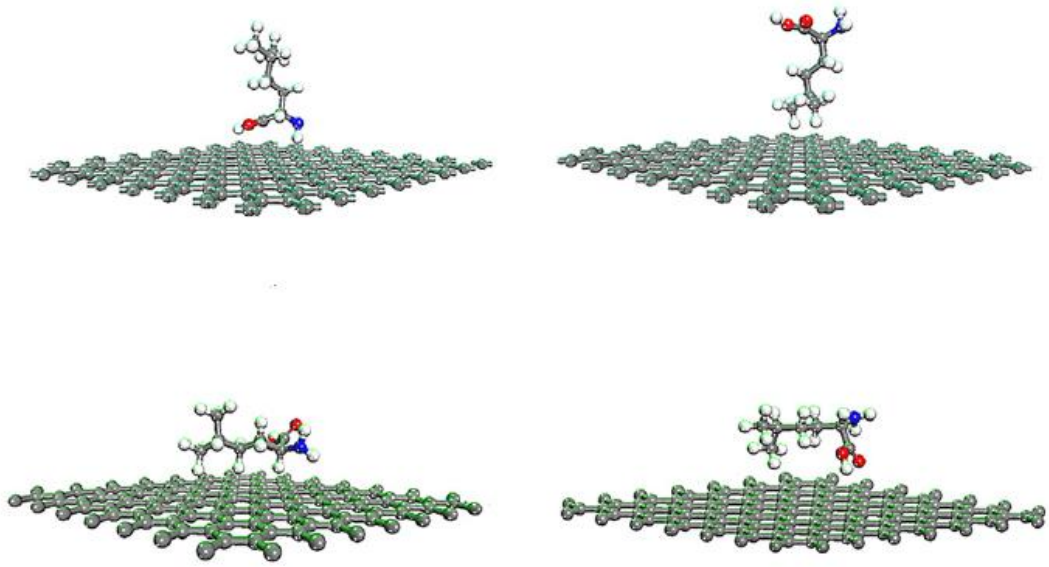

Fig. 2.10 : L-Leucine interacting with graphene surface in four different arrangements.[34]

Thus, it is evident from the aforementioned works that it is very important to dig deep into the interaction mechanisms of Graphene with Biomolecules in order to further tackle the challenges more aptly.

2.5 Bio-conjugate Systems

Nano-structured materials have emerged as the most appealing material for their application in medical diagnostics in the recent years. Nanoparticles such as silica [38] gold [39] and titanium [40] have been exhaustively used as medical diagnostic tool. However, it is of utmost importance to estimate the functional group on the nanoparticle surface for performing the desired activity when it comes to functionalization of nanoparticles.

Given the challenges in biomedical diagnostics, Bio-conjugated Systems have emerged as an important genre of materials for this field [41-48]. Bioconjugation is a chemical approach to form an interface between organic/inorganic composite and biomolecule. Combination of organic and inorganic composites with biomolecules give rise to complex structures with unique properties

constituting that of both the biomolecule and the nanostructure. Inorganic compounds having ionic and covalent interactions provides a wide range of electronic properties like high electron mobility, wide bandgap range such as insulator, semiconductor and metals. In addition, they also have good thermal stability, mechanical hardness, magnetic and dielectric properties.

The ability to tune the electronic properties of bio-conjugated materials at nanoscale has opened a regime of new materials with unique electronic properties totally different from its constituent organic and inorganic components. Furthermore, the nanostructure yields large surface area for interactions comprising biomolecules which offers promising pathway to combine biomolecular functionality.

Such materials with specific features are of particular interest in identification and articulation of biomolecules, protein-nucleic acid interaction, enzyme activity and biometric reactions etc. Since biomolecules are inherent soft molecules and the nanostructures with which it forms the interface are generally hard materials, a controlled precision is required. This helps in having the exceptional properties and also the nature of the biomolecule can be conserved after the interaction with nanomaterial. Due to their peculiar surface chemical heterogeneity, Bioconjugation of DNA, peptides and proteins are one of the most challenging problems.

Thus considerable interest has developed in understanding the interaction between nanostructures and biomolecules [48-57], owing to their unique properties tailored for utilization in detection mechanism and medical diagnostic [58]. Recently, new class of materials for bioconjugation have immerged for applications in medical diagnostics such as nanoparticles [59-60], nanowires [61] and fullerenes [62].

Advantages of these combined systems are: they provide an effective platform developed by DNA decorated carbon nanotube for the higher sensitivity of gases [63] while on the other hand, probing the DNA with conformational changes in its surrounding concentration of ions provide huge possibility to develop great detection mechanism.

For building biosensors, it is needed to explore materials with the following properties:

- High biocompatibility
- Sensitivity
- Selectivity with fast response time
- Feasible nanoscale fabrication.

Considerable theoretical and experimental advances in graphene-based nanomaterials reported changes in electronic transport properties of a graphene sheet, due to covalent or non-covalent forces between graphene and several organic molecules

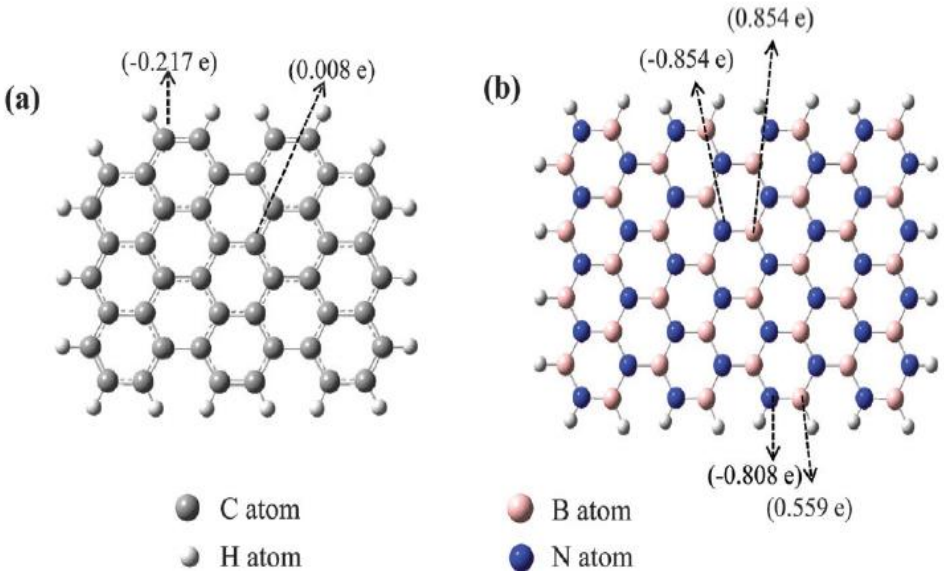

Fig. 2.11 : Optimized geometries of a) graphene and b) BN.[64]

Singla et al. studied the adsorption of three distinct types of amino acids, namely, valine, arginine and aspartic acid, over the surface of graphene and BN nanosheets using DFT. They employed the dispersion correction in the computational methodology, taking into account the long range van der Waals interactions. The adsorption energy values, nearest atom distance and partial charge analysis establish the energetic and physical nature of adsorption on graphene as well as BN nanosheet. The solvation energy and adsorption energy values suggest that the BN sheet is more suitable as an adsorption surface for amino acids.[64]

Luo et al. probed the adsorption of L-cysteine on pristine graphene and B-, N-, Al-, Ni-, Ga-, Pd-doped graphene using DFT calculations. Pristine graphene was reported to physically adsorb L-cysteine whereas N-doped graphene showed physisorption towards the S-end and N-end L-cysteine, and chemisorption towards the O-end radical. On the other hand, Al-, Ni-, Ga- and Pd-doped graphene showed strong chemisorption, with site-specific preference accompanied by several structural changes.[65]

As amino acids play a vital role in living organisms as building blocks of proteins and enzymes,

elucidation of the nature of their interactions with graphene and modified graphene is the focus of the current study.

2.6 Ammino Acid

Amino acids (A.As) are the elementary units of proteins and can reflect the common chemical properties of complicated biomolecules. As proteins play a key role in biology, it is predicted that understanding their interactions with nanomaterials can solve critical problems in the field of biomedicine. For example, investigating the adsorption mechanisms of biomolecules such as proteins on a synthetic surface may give an insight to the reasons for foreign body reaction on the implanted biomaterials.

An amino acid is a compound whose structure contains an amino group and a carboxyl group. α-amino acids are more important in the context of biology. For α-amino acids, the amino group is attached to the α-carbon or the carbon adjacent to the carboxyl carbon. As all amino acids contain an amino group and a carboxyl group, structural differences arise from the variety of R groups that can be present. R groups have varying degrees and types of interaction with the environment and other components. Thus, understanding the chemistry of amino acid side chains is important for understanding the properties of individual amino acids and the proteins they form. Twenty-one amino acids are commonly found in all proteins or polypeptides. Human Body can synthesize some of these amino acids, while the others are obtained via diet. Those obtained from diet are called essential amino acids.

One common method of classifying amino acids is based on their interaction with water. Amino acids are considered hydrophobic, hydrophilic, or ionic. The type of R group present determines whether an amino acid will belong to any of the 3 groups

.Table 2.1: BCAA and their Immune function.[66]

BCAA Mix
●↑ fuel sources for immune cells
●↑immune function of neutrophils and lymphocytes
●↑CD4+, CD4+/CD8+
●↑intestinal immunoglobulins
Isoleucine
●↑excretion of β-defensin
Leucine
●↑ regulation of innate and adaptive immune responses
●↑pro-inflammatory cytokines ↓ anti-inflammatory cytokines
Valine
●↑ dendritic cell function
●↑pro-inflammatory cytokines ↓ anti-inflammatory cytokines

Branched chain amino acids which include leucine, isoleucine and valine, are essential amino acids and must be obtained from the diet. BCAA are considered to be the building blocks for tissue protein accounting for 35% of the essential amino acids in muscle. BCAAs have been extensively used as performance-improvement supplements for body builders and fitness professionals. For example, BCAA were reported to enhance the secretion of insulin . However, increased plasma BCAA levels have also been related to lead to insulin resistance or type 2 diabetes mellitus. One of the possible mechanism for this is the persistent activation of mTOR signalling pathway uncouples the insulin receptor from insulin receptor substrate. Another possible mechanism can be the accumulation of toxic BCAA metabolites may trigger mitochondrial dysfunction which is associated with insulin resistance. BCAA have been also been reported to participate in lipolysis, lipogenesis, glucose metabolism, intestinal barrier function and absorption, glucose transportation, milk quality, mammary health, and immunity. Furthermore, levels of BCAA in the body can act as a biomarker for the early detection of chronic diseases in humans [66].

Density Functional Theory calculation have been employed in order to accurate predict the interaction nature of various substrates/monolayers with amino acids. Larijani *et al.* studied the nature of adsorption of amino acids: Glycine(G), Histidine(H) and Phenylalanine(P) with graphene derivatives

: Pristine Graphene, Defect Induced Graphene and Graphene Oxide. The calculations were done taken into account the dispersive forces using DFT-D2 Grimme's Dispersion Correction within the framework of GGA-PBE. The strongest interactions were noted between the negatively polarized part of the oxidized Graphene and the positively polarized part of the molecules i.e. the hydrogen atoms of the $-NH_2$ and -OH group. Whereas the weakest interactive forces are those between the delocalized Π electrons of the aromatic parts of the molecule and the electron lone pairs of oxygen in oxidized graphene. The adsorption energy on oxidized graphene is in the order H>G>P with that of Glycine/Graphene Oxide highest at -0.85eV.[67]

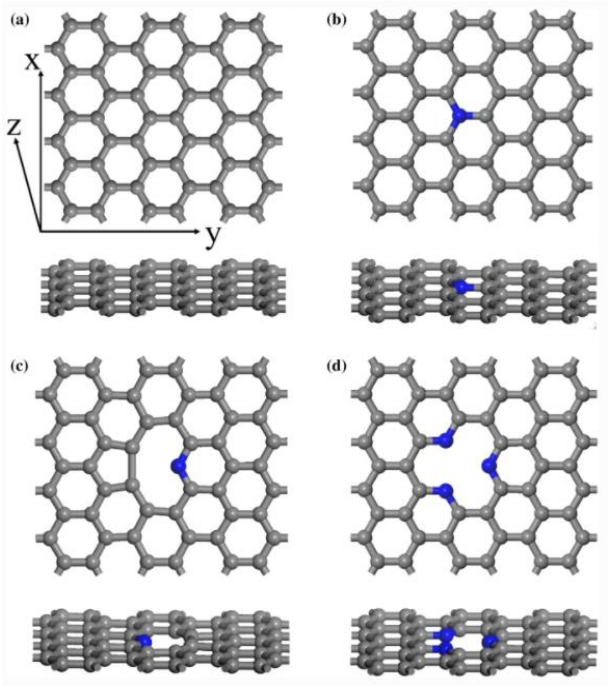

Fig. 2.12: Optimized structures of a) pristine graphene, b) graphitic N, c) pyridinic 1N and d) pyridinic 3N. [68]

Doping has been a very favourable choice in order to modify the properties of the Graphene monolayer and therefore, various modifications of the graphene layer is reported that were evaluated for being used as a potential absorbent for amino acids. N-doped graphene was evaluated to check it's feasibility as a potential sensor for amino acids. Different modifications were done which can be seen from Fig.2.12. The strongest interactions were noticed for Pyridinic N and it was observed that by increasing the Nitrogen content, the polarization was further enhanced resulting in better adsorption.[68]

Graphdiyne(GD) which is a part of the extended Graphene family has also been reported as a promising contender in the game of amino-acid sensing. It consists of sp^2 hybridized hexagonal carbon rings connected by 4 sp hybridized carbon (Fig. 2.13). Calculations in the PBE-D2 showed that single layer GD strongly adsorb amino acids viz. Glycine(G), Glumatic Acid(GU), Histidine(H) and Phenylalanine(P), with respect to Pristine Graphene. The adsorption energies are in the order P>H>GU=G with GD/P having the highest of -1.27eV.[69]

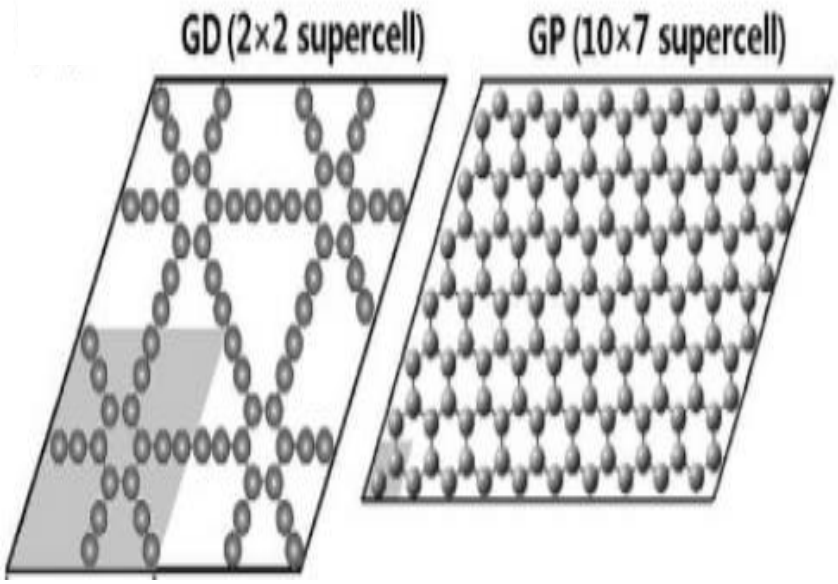

Fig. 2.13: Optimized structures of a) Graphdiyne(GD), b) Pristine Graphene(GP).[69]

2.6.1 Valine Amino Acid

Valine is an aliphatic, extremely hydrophobic essential amino acid in humans and belong to the Branch Chain Aino Acid category. Valine is mostly found in the interior of globular proteins helping to determine three-dimensional structure. Valine, being a glycogenic amino acid, maintains mental vigor, muscle coordination, and emotional calm. In case of sickle-cell disease, a single glutamic acid in β-globin is replaced with valine. As valine is hydrophobic, whereas glutamic acid is hydrophilic, this change makes the hemoglobin prone to abnormal aggregation.

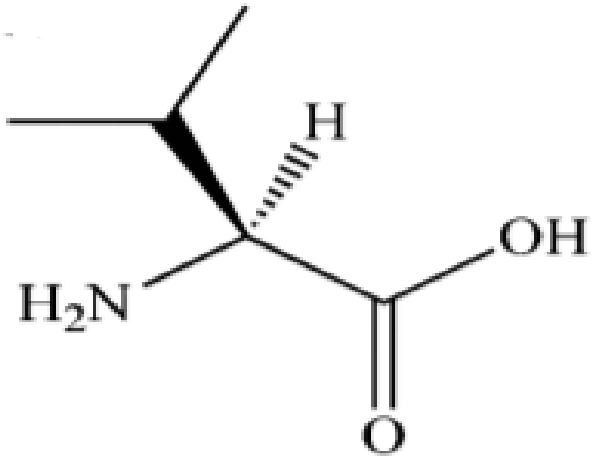

Fig. 2.14 : Chemical structure of valine. [64]

Among Amino Acids(AAs), particularly in the set of essential AAs, Branched-Chain AAs (BCAAs) have been linked with number of disorders, particularly in liver cirrhosis, renal failure, insulin resistance, trauma and cancer. Specifically, high plasma valine concentration is associated with Type

2 Diabetes patients whereas increased extracellular concentration of valine improves dendritic cell function in cirrhosis patients. Stated it's biological significance, the evaluation of valine/modified-graphene bioconjugate systems might unlock potential pathways to device future diagnosis and remediation.

`Considerable amount of work has been done in the past with respect to the interaction phenomenon of Graphene with Amino Acids, Nucleobases and other Organic Molecules. The computational tool is rather useful in providing an insight into the atomic regime of the phenomenon. Valine, given it's biomedical importance, was studied alone with Graphene surfaces and further to enhance the interaction properties with Modified Graphene, viz. Nitrogen doped Graphene[70]. Material Theory groups have tried to investigate the Valine/ Graphene and Valine/ h-BN interactions with more favorable adsorption in the later. [71]

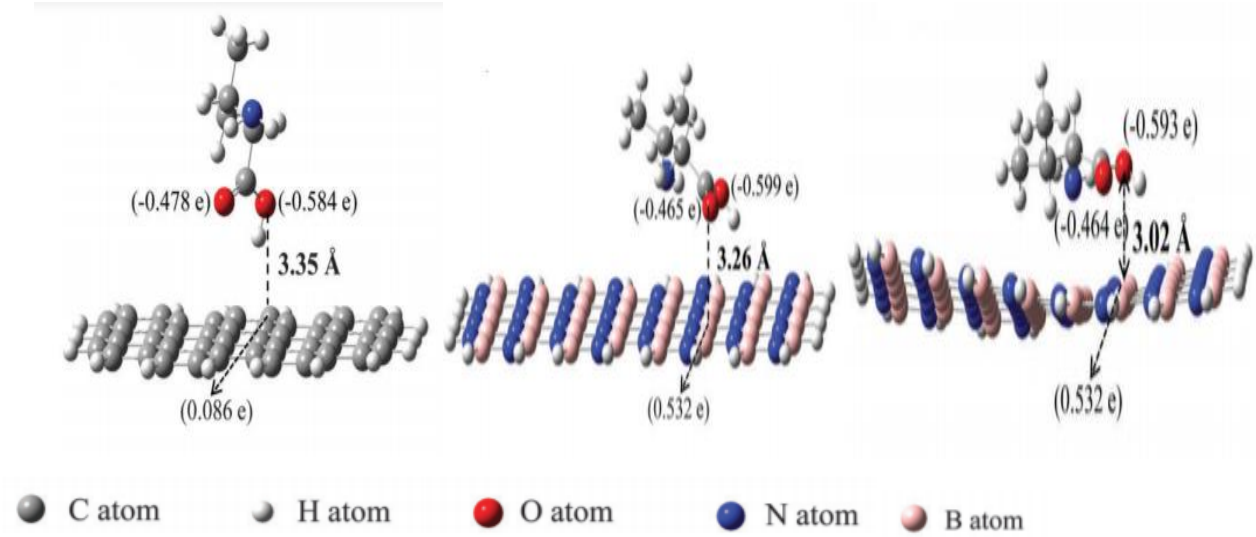

Fig. 2.15: Optimized geometries of valine on graphene, BN sheets and dispersion corrected geometries for BN sheet(left to right). [64]

The adsorption energies for Valine(Val) adsorption on graphene are −89.76 kcal mol^{-1}. The dispersion correction reported negative adsorption energy whereas that without it was positive. This emphasizes the role of van der Waals interactions in the adsorption process. Similar results were obtained for the BN nanosheet as dispersion correction accounted profoundly for the long distance van der Waals interactions by stabilizing the amino acid adsorbed complexes. The adsorption energies

for Val on the BN nanosheet are −161.32 kcal mol^{-1}. The adsorption energy values for valine is larger on the BN nanosheet in comparison to the graphene surface as the polar B–N bond enhances van der Waals interactions by incorporating the dipole–dipole interactions. These results emphasize

the role of dispersion correction while studying adsorption over nano-surfaces and thus indicating that BN nanosheets have a higher affinity towards amino acids in comparison to graphene.[71]

Table 2.2 : Adsorption energy (ΔE_{ad}) values of valine adsorbed on nano-surfaces in gaseous and solvent phases.[64]

System	Adsorption energy (kcal mol^{-1})			
	Without dispersion correction		With dispersion correction	
	Gas phase	Solvent phase	Gas phase	Solvent phase
Val/Gra	−3.65	2.93	−89.76	−81.78
Val/BN	0.97	2.09	−161.32	−158.75

Valine interaction with modified Graphene has also been reported in some literatures though much work has not been carried out in this respect. The Valine/N-doped-Graphene showed more effective adsorption than Pristine Graphene[70]. For this reason, extensive studies need to be carried out in order to understand the interaction mechanisms of modified graphene with valine so that they can be effectively applied to solve some of the most challenging biomedical problems.

CHAPTER 3 : Aim of Present Work

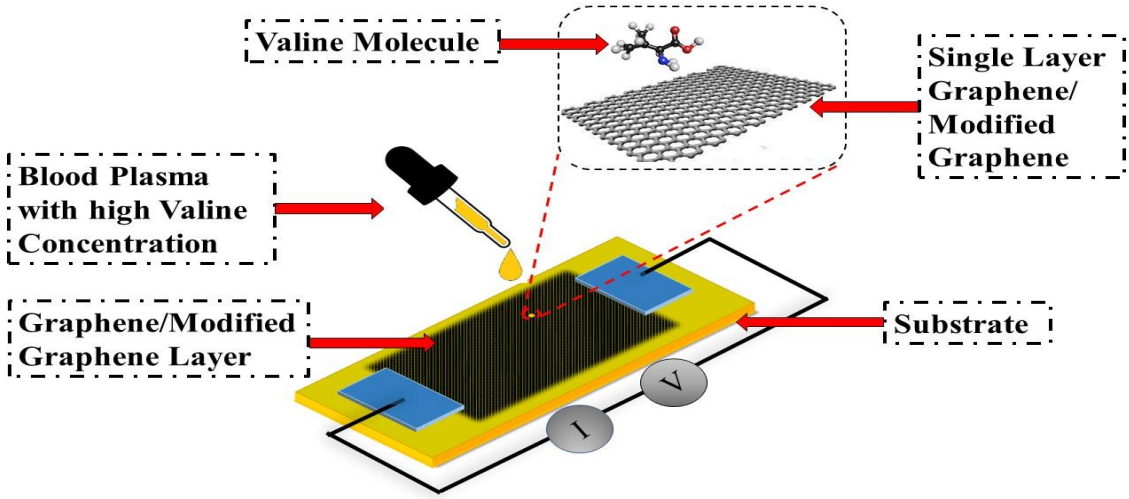

Fig. 3.1 : Schematic of biosensing application of graphene/modified graphene.

The present work aims to investigate the specific interaction (binding) of Valine amino acids with various graphene monolayers such as Doped Graphene, Holey Graphene etc., by using the quantum chemical calculations based on first principle calculations under the frame work of density functional theory. In order to provide the knowledge of underlying physics and chemistry, biomolecule interactions with Graphene monolayers and the complexity of biomolecules will also be discussed. With increased activities in their synthesis, growth, integration in technology and consumer products, there has also been increased concern about their biological and environmental effects. Therefore, as the production and applications of engineered bioconjugated materials continue to increase, it is deemed critically important and timely to develop an understanding of their health and environmental effects, also to unfold new materials. The specific objectives of the present work are following:

1. To obtain a better understanding of the binding mechanism between Modified Graphene nanostructures and biomolecules.
2. To assess the exquisite differences in the adsorption strength of Valine on different graphene nanostructures, which in turn will allow us to understand the interaction.
3. To analyze the results of electronic properties in terms of conducting behavior for possible transport applications and also sensing mechanism of biomolecule over nano surfaces.
4. To develop the new Graphene based nanostructures and finds the possibility of their use as biosensor.

3.1 Choice of Dopant Atom

Literatures have reported the incorporation of various dopant atoms in the graphene monolayer to modify it's physical and chemical properties. Here we propose to calculate the structural, electronic and adsorption properties of Si-doped Graphene to show it's potential use as a biological sensor or drug delivery agent for the essential amino acid : Valine. Reported works show that when Si-atom doped in pristine sheet, the calculated C-Si bond length is about 1.78Å which is greater than that of C-C(about 1.42Å) in pristine form. The increase is length is due to reduced quasi σ bond strength identified by reduced charge density of the C-Si bonds. Distortion of the hexagonal rings of the pristine form results in changed various properties. The doping also opens the zero band gap of pristine graphene evident by the separation of the valence and conduction Dirac points. Si-doped Graphene is reported to act as a Lewis Acid and therefore show strong interactions with lone pair of the functional groups.[72-73]

One of the most important aspect of having doping Silicon and studying it's adsorption properties is due to the fact that Silicon doped Graphene sheet has been successfully synthesized by chemical vapour deposition method[73]. DFT studies have revealed the potential of Si-doped Graphene in catalytic and adsorption properties towards pollutants such as formic acid, N_2O, NO and CO[74-76]. Interaction of Si-doped Graphene with modified nucleobases showed improved adsorption energies with respect to pristine form[77]. Thus, it can be investigated for it's potential use as a biological sensor and drug delivery agent for amino acids as well. Moreover, to the best of our knowledge, adsorption of Valine amino acid has not been studied in details using experimental or computational methods. So here in this work, we study the adsorption behaviour of Valine over Si-doped graphene and pristine graphene computationally to have a comparative view.

CHAPTER 4 : Density Functional Theory

4.1 Origin

Among different computational techniques, one of the most widely accepted methods used for predicting ground state properties of materials with large number of electrons is density functional theory (DFT). In order to solve time-independent Schrödinger like Kohn-Sham equation for studying the properties of bulk, nano materials as well as complex systems of biomolecules-nano materials, DFT proves to be a very efficient tool. It is the developed version of Thomas and Fermi model further treated by Hartree, Fock, Dirac and Slater. DFT was formulated using the two famous theories, one proposed by Hohenberg and Kohn [78] and later by Kohn and Sham [79] which provides an excellent tool for calculating the ground state properties of many electron systems. It is a widely used technique for evaluating the electronic band structure, adsorption and surface defect energy, electric dipole and quadruple moments, etc.

Given the advantage of DFT in it's ability to predict the concerned properties of the materials, there has been a huge surge in DFT based research articles in the recent past and it continues to grow. Considering overall density rather than number density and thus subsequently reducing the 3N degrees of freedom to 3 gives DFT an edge over the rest of the available approaches. Despite such advantages, it must be understood that DFT is unable to provide an exact solution to the Schrödinger equation and therefore various approximations have to be employed. Exchange and correlation functional such as LDA(Local Density Approximation) and GGA(General Gradient Approximation) take into consideration the coulombic interaction and thus increase the efficiency of the calculation.[80-81]

4.1.1 Many Body Problem

At the realms of the atoms, the governing laws applicable is that of Quantum Mechanics. If we want to understand a phenomenon in a material, for example that of adsorption, magnetism etc., we need to understand the interaction behaviour of the fundamental constituents of that material viz. nuclei and electrons. It is due to the interplay between these electrons and ions that all concerned properties of the material emerge. Thus, the behaviour of the fundamental constituents can be understood by solving the time-independent Schrödinger equation [82].

$$\boldsymbol{H\psi = E\psi} \tag{4.1}$$

Here, $\boldsymbol{\psi}$ is the wave function, H is the Hamiltonian of the system and E is the energy eigen value of the system known as total energy of the system. Considering an example, say we need to solve the aforementioned equation for a Hydrogen atom, then it is possible to exactly solve the equation since it's a simple system consisting of one electron and one proton. The energy value for Hydrogen atom is found to be -13.6eV.

But as we move towards complex systems, the problem gets more challenging, considering the large number of electrons and ions. In conventional solids, owing to the sizeable number of electrons and ions, we need to consider the complex interactions between the electrons and ions. Thus, the Hamiltonian of the system also acquires complex form and is given by

$$\boldsymbol{H = T_E + T_I + V_{II} + V_{EE} + V_{IE}} \qquad (4.2)$$

$$\mathbf{H}= -\frac{\hbar^2}{2\,m_e}\sum_i \frac{\partial 2}{\partial \bar{\mathrm{r}}_i^{\,2}} - \frac{\hbar^2}{2\,M_e}\sum_l \frac{\partial 2}{\partial \mathrm{R}_l^{\,2}} + \frac{1}{2}\sum_{\substack{l,l'\\ l\neq l'}} \frac{e^2\ Z_l Z_{l'}}{4\pi\,\varepsilon_0\,|\bar{\mathrm{R}}_l - \mathrm{R}_{l'}|} + \frac{1}{2}\sum_{\substack{i,j\\ i\neq j}} \frac{e^2}{4\pi\,\varepsilon_0\,|\bar{\mathrm{r}}_i - \bar{\mathrm{r}}_j|} - \sum_{\substack{l,l'\\ l\neq l'}} \frac{e^2\ Z_l}{4\pi\,\varepsilon_0\,|\bar{\mathrm{r}}_i - \bar{\mathrm{R}}_l\,|} \qquad (4.3)$$

Here, T_E and T_I are the kinetic energy of electrons and ions, while V_{II}, V_{EE}, and V_{IE} are potential energy of two nuclei, two electrons and nuclei-electron system respectively. In equation 4.3, i and l corresponds to nuclei and electrons respectively; m_e and M are the mass of electron and nuclei respectively; Z_l and $Z_{l'}$ are the charges on different nuclei; and $\bar{r_i}-\bar{r_j}$, $\bar{R_l}-\bar{R_{l'}}$ and $\bar{r_i}-\bar{R_l}$ are the electron-electron, electron-nuclei and nuclei-nuclei distances respectively.

In order to solve the Hamiltonian in equation 4.3, we require the charge of electrons, mass of electron and nuclei and the distances and thus, there are no adjustable parameters in the equation. Since the calculation is from the very fundamentals considering the aforementioned parameters, it is known as " First Principle Calculations". Thus, solving equation 4.2 with the calculated value of Hamiltonian from 4.3, we get the energy eigen value also known as the total energy of the system and thereafter from the calculated total energy, we find the ground state properties of the concerned material at equilibrium.

In practice, as we move from smaller simpler systems that of hydrogen atom to larger more complex systems, it becomes increasing difficult to solve the Schrödinger equation since the number of complex interactions to be taken into count increases as the number of electrons and ions increases. Therefore, in order to solve the complexity, we employ different approximations which tries to reduce the complexity of the problem.

4.2 Wave Function Based Method To Solve Many-Body Equation

4.2.1 Born-Oppenheimer Approximation

Since Ions are 10^3 -10^4 times heavier than electrons, we can consider the ions to be stationary with respect to electrons. In Born-Oppenheimer (BO) approximation, the wave function is separated in two parts: (a) electronic part and (b) ionic part. Considering the BO approximation, many body wave function can be expressed as [83]

$$\boldsymbol{\psi} = \boldsymbol{\chi_i}\,(\bar{R})\;\boldsymbol{\Psi_E}\,(\bar{r},\bar{R}) \tag{4.4}$$

Here, $\Psi_E\ (\bar{r},\ \bar{R})$ stands for electronic wave function whereas $\chi_i\ (\bar{R})$ represents ionic wave function.

$$\left[-\frac{\hbar^2}{2\,M_e}\sum_i \frac{\partial 2}{\partial \mathrm{R}_i^{\,2}} + \mathrm{V_{II}}(\bar{\boldsymbol{R}}) + \mathrm{E_E}\ (\bar{\boldsymbol{R}})\ \right]\boldsymbol{\chi_i}(\bar{\boldsymbol{R}}) = \mathrm{E}\ \boldsymbol{\chi_i}(\bar{\boldsymbol{R}}) \tag{4.5}$$

$$\left[-\frac{\hbar^2}{2\,m_e}\sum_i \frac{\partial 2}{\partial \bar{\mathrm{r}}_i^{\,2}} + \mathrm{V_{IE}}(\bar{\boldsymbol{r}},\bar{\boldsymbol{R}}) + \mathrm{V_{EE}}\ (\bar{\boldsymbol{r}})\ \right]\boldsymbol{\psi_E}(\bar{\boldsymbol{r}},\bar{\boldsymbol{R}}) = \mathrm{E_E}\,\boldsymbol{\psi_E}\ (\bar{\boldsymbol{r}},\bar{\boldsymbol{R}}) \tag{4.6}$$

Separating the electronic and ionic parts of the wave function we get the above equations 4.5 and 4.6. Since the ions are stationary, the kinetic energy of the ions are not considered. The ion-ion potential becomes constant and the electron-ion interaction depends only on the position of the electrons.

4.2.2 Hartree Approximation

In Born-Oppenheimer(BO) Approximation, the wave function was separated into electronic and ionic part. Thereafter, Hartree proposed an approximation considering only the electronic wave function and represented that in terms of single particle function.[84]

$$\boldsymbol{\Psi_H} = \boldsymbol{\Psi}(\bar{r}_1,\boldsymbol{\sigma}_1)\,\boldsymbol{\Psi}(\bar{r}_2,\boldsymbol{\sigma}_2)\,\boldsymbol{\Psi}(\bar{r}_3,\boldsymbol{\sigma}_3)\ldots\ldots\ldots\ldots\,\boldsymbol{\Psi}(\bar{r}_N,\boldsymbol{\sigma}_N) \tag{4.7}$$

Where $\boldsymbol{\Psi}(\bar{r}_i,\boldsymbol{\sigma}_i)$ represents the wave function of the i^{th} electron and $\bar{r}_i$ represents the position coordinates of the i^{th} electron with spin $\boldsymbol{\sigma}_i$.

Now, substituting the value of the Hamiltonian from equation 4.6 and the wave function from 4.7, it is possible to write the Schrödinger equation for the electronic part.

$$-\frac{\hbar^2}{2\,m_e}\nabla^2{}_i\,\boldsymbol{\psi}_{\mathbf{E}} - \frac{1}{4\pi\,\varepsilon_0}\sum_l \frac{Ze^2}{|\bar{\mathbf{r}}_i - \mathbf{R}_l|}\boldsymbol{\psi}_{\mathbf{i}} + \frac{1}{4\pi\,\varepsilon_0}\sum_{j\neq i}\int \frac{e^2\,|\psi_i|^2}{|\bar{\mathbf{r}}_i - \bar{\mathbf{r}}_j|}\,\mathbf{d}^3\mathbf{r}_\mathbf{j} = \in_i \boldsymbol{\Psi}_i \quad (4.8)$$

On the left-hand side of the above equation, the first term represents the kinetic energy and the next two terms are the ion-electron potential(V_{IE}) and Hartree potential(V_H) respectively. Here, the V_{IE} depends only on the position of the electrons. The above equation is known as the Hartree equation, and the solution of this gives the exact ground state energy by minimizing the expected energy value.

$$\mathbf{E} = \frac{\langle \psi_\mathbf{H} |\, \mathbf{H} \,|\, \psi_\mathbf{H} \rangle}{\langle \psi_\mathbf{H} \,|\, \psi_\mathbf{H} \rangle} \quad (4.9)$$

Thus, the Hartree approximation is instrumental in breaking down the many-body problem into a single electron one and therefore is also known as the independent electron approximation. However, there are some drawbacks of this approximation. It neglects the correlations between the electrons and does not consider the asymmetric wave function for the electrons. According to the Pauli's exclusion principle, as electrons are considered as Fermions, their asymmetric nature must be considered.

4.2.3 Hartree-Fock Approximation

In order to take into consideration the asymmetric nature of wave function and the effect of correlation, Hartree and Fock formulated the asymmetric wave function given by the equation below:

$$\boldsymbol{\Psi_{HF}}(\bar{\boldsymbol{r}}_1, \boldsymbol{\sigma_1}, \dots, \bar{\boldsymbol{r}}_i, \boldsymbol{\sigma_i}, \dots, \bar{\boldsymbol{r}}_j, \boldsymbol{\sigma_j}, \dots) = -\boldsymbol{\Psi_{HF}}(\bar{\boldsymbol{r}}_1, \boldsymbol{\sigma_1}, \dots, \bar{\boldsymbol{r}}_i, \boldsymbol{\sigma_i}, \dots, \bar{\boldsymbol{r}}_j, \boldsymbol{\sigma_j}, \dots) \quad (4.10)$$

The approximation calculates the minimum energy from 4.9 considering the determinant form of the asymmetric wave function known as Slater's determinant[84]:

$$\boldsymbol{\Psi_{HF}}(\bar{\boldsymbol{r}}_1, \boldsymbol{\sigma_1}, \dots, \bar{\boldsymbol{r}}_\mathbf{N}, \boldsymbol{\sigma}_\mathbf{N}) = \begin{vmatrix} \boldsymbol{\psi_1}(\bar{\mathbf{r}}_1, \boldsymbol{\sigma_1}) & \boldsymbol{\psi_1}(\bar{\mathbf{r}}_2, \boldsymbol{\sigma_2}) \dots\dots\dots & \boldsymbol{\psi_1}(\bar{\mathbf{r}}_N, \boldsymbol{\sigma}_N) \\ \boldsymbol{\psi_2}(\bar{\mathbf{r}}_1, \boldsymbol{\sigma_1}) & \boldsymbol{\psi_2}(\bar{\mathbf{r}}_2, \boldsymbol{\sigma_2}) \dots\dots\dots & \boldsymbol{\psi_2}(\bar{\mathbf{r}}_N, \boldsymbol{\sigma}_N) \\ \boldsymbol{\psi_N}(\bar{\mathbf{r}}_1, \boldsymbol{\sigma_1}) & \boldsymbol{\psi_N}(\bar{\mathbf{r}}_2, \boldsymbol{\sigma_2}) \dots\dots\dots & \boldsymbol{\psi_N}(\bar{\mathbf{r}}_N, \boldsymbol{\sigma}_N) \end{vmatrix} \quad (4.11)$$

The determinant of the wave function can be written as

$$\boldsymbol{\Psi_{HF}} = \frac{1}{N!}\sum_\mathrm{P} (-\mathbf{1})^{\,p}\boldsymbol{P}\,\boldsymbol{\Psi_1}(\boldsymbol{x_1})\,\boldsymbol{\Psi_2}(\boldsymbol{x_2}) \dots \boldsymbol{\Psi N}(\boldsymbol{x}_N) \quad (4.12)$$

Where, x = ($\bar{\mathrm{r}}$, σ), P is the permutation number and p is number of interchanges making up this permutation. The expected value of the Hamiltonian can be obtained by substituting the determinant in equation 4.9:

$$E = \sum_i \int \psi*(\vec{r}) \left[-\frac{\hbar^2}{2\,m_e} \nabla^2{}_i + V_l(\vec{r}) \right] \psi(\vec{r})\, d^3r + \frac{1}{2} \sum_i \sum_{j \neq i} \int \int \frac{e^2\, |\psi_i(x_i)|\ |\psi_j(x_j)|^2}{|\vec{r} - \vec{r}'|} d^3r d^3r'$$

$$- \frac{1}{2} \sum_{i,j} \sum_{j \neq i} \int \int \frac{e^2\ \psi_i(\vec{r}'')\, \psi_j(\vec{r})\ \ \psi_i^*(\vec{r}')\ \ \psi_j^*(\vec{r})}{|r^{\rightarrow} - \vec{r}'')} d^3r d^3r' \qquad (4.13)$$

The first term on the left hand side of the above equation represents the kinetic energy and external potential interaction, the middle term represents the Hartree potential(V_H) and the last term appears due to the Pauli's exclusion principle also known as the exchange energy. Equation 4.13 can be minimized leading to the canonical form of the Hartree-Fock equation:

$$[-\frac{\hbar^2}{2\,m_e} \sum_i \nabla^2 - V_l(r^{\rightarrow}) + V_H(r^{\rightarrow})] \Psi_i(r^{\rightarrow})$$

$$-\frac{1}{2} \sum_{i,j} \sum_{j \neq i} \iint \frac{e^2\ \Psi_j^*(r^{\rightarrow\prime}) \Psi_i^*(r^{\rightarrow\prime}) \Psi_j^*(r^{\rightarrow})}{4\pi\, \varepsilon_0\, |r^{\rightarrow} - r^{\rightarrow\prime}|} d^3r\, d^3r', j = \in_i \Psi_i(r^{\rightarrow}) \qquad (4.14)$$

The Hartree approximation thus improves when taken into consideration the asymmetric nature of the wave function but the total energy $\in_i$ contains minimization over sum of the slater determinant containing N particle. Solving such large determinant requires high computational time and therefore are very costly.

4.3 Density Functional Theory: Density Based Method

In order to understand the properties of materials, it is necessary to understand the interaction of it's fundamental constituents and therefore, we try to solve the time independent Schrödinger equation to understand the interaction behaviour of the electrons and ions. Thus, the total energy of the ground state of the electrons is required to be found by solving the equation 4.6. but the solution of the equation becomes very complex as for N electrons there are 3N variables. Therefore, in order to overcome this, a density based method was proposed in which the interaction energy depends only on the density of the electrons.

4.3.1 Thomas and Fermi Theory

The idea of calculating the ground state energy of electrons using density based methods were first proposed by Thomas and Fermi(TF).[85-86] In 1927,the duo proposed a way to formulate the total

energy of the system using the functional of electron density rather than single particle wave function. Using electron density as the basic variable, TF theory is able to predict the kinetic energy of N interacting electrons from the following equation:

$$T_{TF}=C_k\int n \quad (\bar{r})^{5/3} d^3r \tag{4.15}$$

Where $C_k=\frac{3\hbar^2}{10\, m_e}\ (3\,\pi^2)^{2/3} n(\bar{r})$ is the density of electrons. T_{TF} is the local approximation to the kinetic energy that can be obtained by summation of all the free electron energy states up to Fermi wave vector. TF theory gives the total energy in equation 4.16 as a functional of electron density by adding kinetic energy, electrostatic energy and interaction of external potential.

$$E=T_{TF}+\int V_{IE}(\bar{r})\, n(\bar{r}) d^3r+\frac{1}{2}\iint \frac{e^2 n(\vec{r'})\, n(\vec{r})}{4\pi\, \varepsilon_0 |\vec{r}-\vec{r'}|}\, d^3r d^3r' \tag{4.16}$$

This energy is known as Thomas-Fermi energy and the TF equation can be obtained by minimizing the energy by a constraint – Lagrange multiplier μ which gives the appropriate number of particles.

$$\frac{5}{3}C_k n(\bar{r})^{2/3}+\int e^2\, 4\pi\varepsilon\, \varepsilon_0\, n(\vec{r'})|\vec{r}-\vec{r'}|d^3r'=\mu$$

$$\mu=\frac{5}{3}C_k n(\bar{r})^{2/3}+V(\bar{r}) \tag{4.17}$$

This the basic equation of the TF theory and can be solved self-consistently. The TF equation here doesn't take into consideration the exchange energy and was modified by Dirac in which he included the exchange interaction. Also the TF theory doesn't show any shell structure and fails to describe the behaviour of electrons for atoms in complex systems.

4.3.2 Hohenberg and Kohn Theory

In this section, we describe the two basic theorems of DFT given by Hohenberg and Kohn [78]. They showed that all the ground state properties of systems with many electrons can be calculated as a functional of electron density. Functional is a function of function that maps to a number i.e. path for function to a finite number. The complexity of the calculations are reduced since the density of

electrons depend on only three variables.

Theorem 1: *The external potential V(r) is a unique functional of electron density n(r). As a result, the total ground state energy E of any many-electron system is also unique functional of n(r),* $\boldsymbol{E = E[n]}$.

An unique Hamiltonian can be obtained from the external potential corresponding to the density of electrons and can therefore be used to solve the many electron Schrodinger equation.

In order to have a better understanding of the above theorem, let's consider two external potentials $V_{ext}^{(1)}(\mathbf{r})$ and $V_{ext}^{(2)}(\mathbf{r})$ which differ by a constant and give the same density n(r). These two potentials will give rise to two unique Hamiltonians and wave functions viz. $H^{(1)}$ and $H^{(2)}$; $\psi^{(1)}_{ext}(\boldsymbol{r})$ and $\psi^{(2)}_{ext}(\boldsymbol{r})$ respectively.

Considering the variational principle, it can be stated that $\psi^{(2)}_{ext}(\boldsymbol{r})$ cannot be the ground state of $H^{(1)}$ and therefore:

$$\mathbf{E^{(1)}} = \langle \boldsymbol{\Psi^{(1)}} | \boldsymbol{H^{(1)}} | \boldsymbol{\Psi^{(1)}} \rangle < \langle \boldsymbol{\Psi^{(2)}} | \boldsymbol{H^{(1)}} | \boldsymbol{\Psi^{(2)}} \rangle \tag{4.18}$$

Making things simpler, we consider the non-degenerate system[88]. From equation 4.18, the last term can be written as:

$$\langle \boldsymbol{\Psi^{(2)}} | \boldsymbol{H^{(1)}} | \boldsymbol{\Psi^{(2)}} \rangle = \langle \boldsymbol{\Psi^{(2)}} | \boldsymbol{H^{(2)}} | \boldsymbol{\Psi^{(2)}} \rangle + \int \boldsymbol{dr}[\boldsymbol{V_{ext}^{(1)}(r) - V_{ext}^{(2)}(r)}]\boldsymbol{n_0(r)} \tag{4.19}$$

Similarly, we can write the equation for $H^{(2)}$:

$$\langle \boldsymbol{\Psi^{(1)}} | \boldsymbol{H^{(2)}} | \boldsymbol{\Psi^{(1)}} \rangle = \langle \boldsymbol{\Psi^{(1)}} | \boldsymbol{H^{(1)}} | \boldsymbol{\Psi^{(1)}} \rangle + \int \boldsymbol{dr}[\boldsymbol{V_{ext}^{(2)}(r) - V_{ext}^{(1)}(r)}]\boldsymbol{n_0(r)} \tag{4.20}$$

Adding the two aforementioned equations 4.19 and 4.20, we get:

$$\boldsymbol{E^{(1)} + E^{(2)} < E^{(2)} + E^{(1)}} \tag{4.21}$$

This proves that the initial guess of considering two different external potentials giving the same electron density value is false and therefore, establishes the theorem.

Theorem 2: *The functional $E[n]$ for the total energy has a minimum equal to the ground state energy at the ground state density.*

Electron density is used to determine the external potential which is unique and thereafter can be used for calculating the electronic wave function and other observables. Every other term can therefore be represented in terms of density and the total energy can be written as:

$$\boldsymbol{E[n]=T[n]+E_{int}[n]+\int V_{ext}(r)n(r)+E_{II}\equiv F[n]+\int V_{ext}(r)n(r)+E_{II}} \quad (4.22)$$

Here, F[n] represents the interaction potential and kinetic energy of the electrons for all systems. The ground state energy can be calculated using the unique ground state density:

$$\boldsymbol{E^{(1)}=E[n^{(1)}]=\langle\Psi^{(1)}|H^{(1)}|\Psi^{(1)}\rangle} \quad (4.23)$$

The total energy here can be written as a functional of n(r). F[n] can also be stated in terms of n(r) as a functional.

$$\boldsymbol{F[n]=T_s[n]+\frac{1}{2}\iint \frac{e^2 n(\vec{r'})\, n(\vec{r})}{4\pi\,\varepsilon_0 n|\vec{r}-\vec{r'}|} d^3r\, d^3r' + E_{XC}[n]} \quad (4.24)$$

Thus by knowing F[n], we can now vary the density until the total energy minimization of the system is achieved. The knowledge of the total energy of the system is therefore sufficient to calculate the ground state energy and density.

4.3.3 Kohn-Sham Equation

The Hohenberg and Kohn approach is just the restructuring of many body interacting systems in terms of electron density. HK theory approximated kinetic energy of electrons and exchange-correlation energy in the same way as TF theory. In order to handle the kinetic energy in a much better way, Kohn and Sham (KS) replaced the potential of interacting system by an auxiliary non-interacting system with assumption of same ground state density and then same ground state properties [79]. For this groundbreaking work, Walter Kohn was awarded Noble prize in chemistry in 1998.

In this approach, the kinetic energy term is separated from equation 4.24 which results in the following equation:

$$\boldsymbol{E[n(\bar{r})]=\int V(\bar{r})n(\bar{r})d^3r\ T_s[n]+\frac{1}{2}\iint \frac{e^2 n(\vec{r}')\, n(\vec{r})}{4\pi\,\varepsilon_0 n|\vec{r}-\vec{r}'|}d^3r d^3r'+E_{XC}[n]} \quad (4.25)$$

Here, in the above equation the kinetic energy $\boldsymbol{T_s[n]}$ is an independent term and $\boldsymbol{V(\bar{r})}$ replaces $\boldsymbol{V_{ext}(\bar{r})}$ which is the potential between the nuclei and the electrons.

The quantum mechanical effect in many body system is taken into account by the exchange correlation energy $\boldsymbol{E_{XC}[n]}$.

$$\frac{\delta E[n]}{\delta n(\vec{r})} - \boldsymbol{\mu} = 0 \quad (4.26)$$

$$\frac{\delta T_s[n]}{\delta n(\vec{r})} + \boldsymbol{V(\bar{r}) + V_H(\bar{r}) + V_{XC}(\bar{r}) - \mu} = 0 \quad (4.27)$$

In the above equation(4.27), the Hartree potential ($V_H(\bar{r})$) is given in terms of electron density and $V_{XC}[n]=\frac{\delta E_{XC}[n]}{\delta n(\vec{r})}$. The solution of the equation gives the electron density using which we can calculate the total energy of the system. Thus, the equation has two unknown terms: the kinetic energy term $\boldsymbol{T_s[n]}$ and the exchange correlation energy term $\boldsymbol{E_{XC}[n]}$.

In the Kohn-Sham theory, the density was assumed to be the square of the orbitals of the system where $|\psi_j(\vec{r})$ determine the KS orbitals :

$$\mathbf{n(\bar{r}) = \sum_{i=1}^{N} |\psi_j(\vec{r})|^2} \quad (4.28)$$

The KS energy for a single particle can be formulated into the following equation:

$$\mathbf{T_s[n] = -\frac{\hbar^2}{2\,m_e}\sum_i^N <\psi_i(\vec{r})\,|\,\nabla^2\,|\,\psi_i(\vec{r})> = -\frac{\hbar^2}{2\,m_e}\nabla^2} \quad (4.29)$$

$T_s[n]$ in the above equation represents the oscillations of the shell structure and contains a large part of the total kinetic energy. $\boldsymbol{E_{xc}[n]}$ here signifies the summation of the electronic exchange correlation energy : $\boldsymbol{E_{xc}[n]= E_x[n]+E_c[n]}$. $\boldsymbol{E_x[n]}$ is the slater determinant and therefore by solving 4.25, we get:

$$-\frac{\hbar^2}{2\,m_e}\nabla^2 + V_{eff}(\vec{r})]\,\Psi_i(\vec{r}) = \in_i \Psi_i(\vec{r}^{\,\rightarrow}) \qquad (4.30)$$

The effective potential $V_{eff}(\vec{r})$ is determined by the summation of exchange potential ($V_{ext}(\vec{r})$), Hartree potential $V_H(\vec{r})$ and exchange correlation potential ($V_{XC}(\vec{r})$). The above formulation is known as the Kohn-Sham equation. Solving the KS equation gives exact ground state energy of the system describing the behaviour of an electron moving in a many-electron system by the help of an effective potential. Since the solution of the equation depends on only 3 variables it significantly reduces the computational cost and thus, KS theory is regarded as one of the most powerful tool for determining the ground state energy.

The only drawback of this theory is that the exact form of the exchange correlation energy functional is still not unknown. Therefore, different approximations are taken into account while solving the equation such as Local Density Approximation(LDA) and Generalized Gradient Approximation(GGA).

4.3.4 Self-Consistency in KS Equation

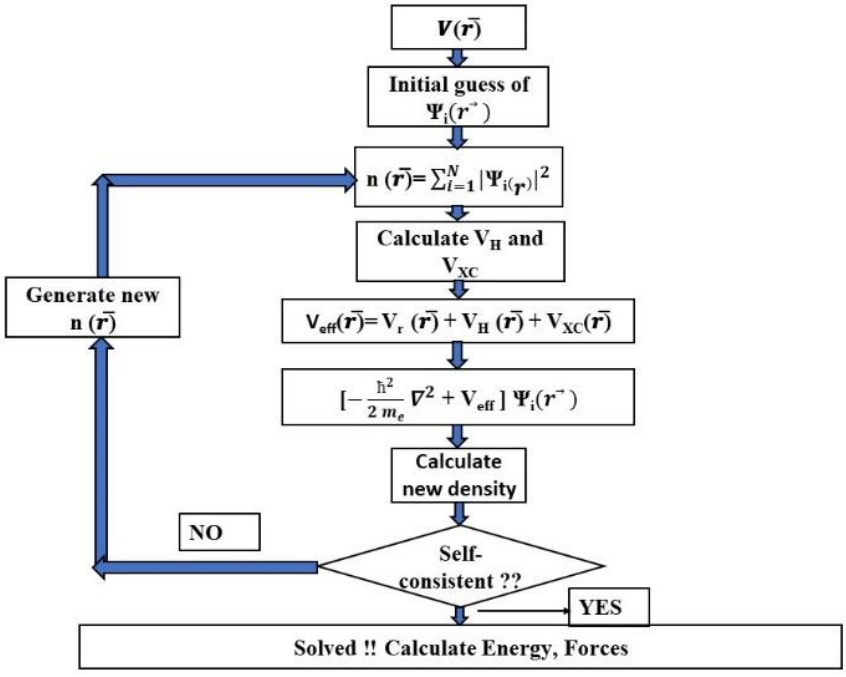

Fig. 4.1: The flowchart of Self Consistency calculation.[source: DFT Tutorial]

The solution to the KS equation in practice is done by changing the density of electrons and effective

potential to achieve self-consistency. The above figure represents the flow diagram of self-consistency calculation to solve the KS equation. In order to solve the KS equation we need to know the effective potential. The exchange correlation and Hartree potential depends on the electron density. With the initial guess of the density, we try to estimate the correlation energy. By adding up the energy of isolated atoms in a system, we approximate the initial guess for the density.

After calculating the effective potential, the unknown wave function $\boldsymbol{\Psi i}(\bar{\boldsymbol{r}})$ is used to determine the new density. Initial guess for the electron density is made in the self-consistency calculation and thereafter if the old density is equal to the new calculated density then the calculation is said to be self-consistent. The total energy is then calculated using the following equation:[88]

$$\mathbf{E[n]} = 2\sum_{v=1}^{N_{e/2}} \epsilon_v - \frac{e^2}{2}\int \frac{\mathbf{n(r)n(r')}}{|\mathbf{r}-\mathbf{r}'|}\,\mathbf{dr\,dr'} + \boldsymbol{E_{xc}[n]} - \int \boldsymbol{drn(r)V_{xc}(r)} + \boldsymbol{E_{Ewald}} \quad (4.31)$$

$\mathbf{E^E_{wald}}$ is the nuclei-nuclei interaction energy.

4.4 Exchange and Correlation Functional

DFT solves many body problem using KS equation taking into consideration different approximation for exchange and correlation potential. Various types of approximation such as LDA, GGA, meta-GGA etc. have been taken for this potential [79]. The exchange interaction term is given as

$$\boldsymbol{E_x}\,[\boldsymbol{n}] = \langle \boldsymbol{\Psi}[\boldsymbol{n}]|\boldsymbol{V_{EE}}|\boldsymbol{\Psi}[\boldsymbol{n}]\rangle - \boldsymbol{U}[\boldsymbol{n}] \quad (4.32)$$

It is the repulsion between electrons and is calculated from KS wave function, which further gives the Hartree contribution and exchange interaction. The Ks equation is evaluated using the slater determinant and the Fock orbitals give the exchange energy. KS DFT and HF exchange energy differ in very fine lines and they are considered to be from two different sources:

1) While KS exchange energy for a defined system is the exchange of the KS orbitals evaluated on the exact density, on the other hand HF exchange is evaluated on the basis of HF orbitals.

2) In order to eliminate the difference in density, the KS exchange energy with that from HF, the difference in the terms being only due to the local potential on the KS orbitals.[89]

The correlation term is therefore:

$$\boldsymbol{E_c[n]=F[n]-T_s[n]-U[n]-E_X[n]} \quad (4.33)$$

Exact formalism of exchange correlation term is still unavailable and therefore, various approximations are taken into account depending the system that is being treated.

4.4.1 Local Density Approximation (LDA)

With the assumption that the electron density varies very slowly in space and that the electron gas in a small volume element (d^3r) can be considered locally uniform, Kohn and Sham formulated the first approximation known as the Local Density Approximation or LDA. LDA is very useful in predicting the electronic band structure of solids and molecules. Thus, using the exchange correlation of the homogeneous gas, the value of the term E_{XC} can be evaluated.

$$E_{XC}^{LDA}[n(r)] = \int \mathrm{dr\ n(r)}\ \epsilon_{XC}^{LDA}\ [n(r)] \quad (4.34)$$

$$V_{xc} = \left(E_{xc}[n] + n\ \frac{\boldsymbol{\delta E_{xc}[n]}}{\boldsymbol{\delta n}} \right) \quad (4.35)$$

In the above equation, $E_{xc}[n]$ gives the LDA exchange correlation per electron in a homogeneous electron gas with density n.

Systems in which electrons are placed in infinite region of space, uniform positive external potential LDA works out to be a good approximation. Given it's advantages in various calculations, LDA suffers from some drawbacks. It fails in strongly correlated systems such as that of transition metals also found to overestimate binding energy in calculations related to quantum chemistry. LDA fails in calculations pertaining to systems containing odd number of electrons since it is unable to differentiate between polarized and unpolarized electron densities.

4.4.2 Generalized Gradient Approximation(GGA)

The electron density, in case of complex systems, tend to vary with respect to the volume element and therefore, the Local Density Approximation(LDA) fails to predict the ground state energy of

such systems. The Generalized Gradient Approximation or GGA which was proposed in order to overcome the drawbacks of LDA, not only considered the density but also accommodated the gradient of the density for evaluating the exchange-correlation term. [90]

$$E_{XC}^{LDA}[n(r)] = \int \mathrm{dr\ n(r)}\ \epsilon_{XC}^{LDA}\ [n(r)]\ ,\boldsymbol{\nabla n(r)},\ldots) \tag{4.36}$$

Exchange-correlation is the semi-empirical from and the degree of non-locality depends on the electron density. Density inhomogeneity is favoured by GGA more than LDA and thus the approximation assumes a gradient in charge density.

$$\boldsymbol{E_{xc}[n]=\int \varepsilon_{xc}(n)|_{n=n(r)} n(r) F_{xc}[n(r),\nabla n(r)]dr} \tag{4.37}$$

Simplification of the calculation requires the E_{XC} and F_{XC} to be parameterized analytic functions. From first principle calculations, Perdew, Burke and Ernzerhof (PBE)[91] were able to parameterize E_{XC} and $F_{XC.}$ Perdew-Wang(PW91)[92] was instrumental in designing an analytical fit to this numerical GGA

4.4.3 Pseudopotentials

In order to simplify calculations, DFT can be performed by explicitly defining the valence electrons only. This method can be achieved using the *"pseudopotentials"*. Since the core electrons are tightly bond with the nucleus unlike the valence electrons which tend to localize further away, they appear as electrons in an isolated atom.[93] Thus, it is possible to perform DFT calculations considering the core electrons to be fixed and therefore not describing their wave functions. Furthermore, it is also possible to completely neglect the core electrons, thus saving computational time and cost. Depending on the level of accuracy that is required to achieve, the separation between the core and the valence electrons can be done.

Elimination of the core electrons requires careful scrutiny. Starting from near the nucleus, the valence electronic wave functions must undergo a sign change in order to be orthogonal to the core states.

Completely eliminating the core electrons would result in the valence electrons not exhibiting the proper "nodal structure" near the nucleus. Also it would be difficult to describe the states in a real-space grid or plane wave basis even if proper oscillating features could be obtained in the wave

functions.

Inappropriate description of the oscillating part of the wave function could lead to inaccuracy in calculation. The solution to this could be using a fine real-space grid or having a high kinetic energy cutoff for the plane wave basis. But this would lead to time-consuming calculations. Thus, in order to overcome the difficulties of the nodal structure of the valence wave function, it would be beneficial to replace the oscillating part with a smooth and node-less curve : which is generally reffered to as the “all electron wave function”.

The pseudo wave function however solves all the problems related to the nodal structure of the all-electron wave function. The idea behind the pseudopotential method is to define a modified nuclear potential that satisfies the following:

1) Outside the pseudized region, the potential match the original KS potential.
2) Inside the region, it should be such that the solution of the KS equation exactly yields the pseudopotential.

Mainly there are two types of pseudopotentials: Normal conserving and Ultrasoft. The ultra-soft pseudopotential provides accurate calculations by expressing the problem in terms of a smooth and auxiliary function around each ionic core.

4.5 Dispersion Correction in Density Functional Theory

The advantage of using Kohn – Sham DFT to study the electronic structure of materials is attributed to it’s ability to provide distinct properties of molecules and solids with reasonably accurate predictions. LDA, GGA and hybrid functional are taken into account to describe the exchange correlation energy. Despite such approximations, both GGA as well as hybrid functionals failed to consider the van der Waals (vdW) forces which arise due to the long-range electron interactions.[94-98] Therefore, in order to incorporate the van der Waals force, the term $\boldsymbol{E_{disp}}$ is added and the total energy is given by

$$\boldsymbol{E_{DFT-D}} = \boldsymbol{E_{KS-DFT}} + \boldsymbol{E_{disp}} \tag{4.38}$$

where E_{DFT-D} is general KS self-consistency energy.

CHAPTER 5 : Interaction of Valine with Modified Graphene: A Dispersion Corrected Density Functional Theory Calculations

Using the DFT-D2 method, i.e. Density Functional Theory method within the GGA-PBE framework employing Grimme's Dispersion Correction, we study the interaction behaviour of Essential Amino Acid: Valine on Silicon doped Graphene in comparison to the Pristine Graphene surface to unlock it's potential use as a biosensor.

5.1 Computational Methods

The calculations in this study were performed using the Density Functional Theory(DFT) based on first principle approach with a plane wave ultrasoft pseudopotential method implemented in Quantum Espresso code.[99] Broyden-Fletcher-Goldfarb-Shanno algorithm (BFGS) was used to relax all the ground state parameters of all the structures. Perdew-Burke-Ernzerhof (PBE) parameterized energy was used in the Generalized Gradient Approximation (GGA) to incorporate the exchange correlation functional.

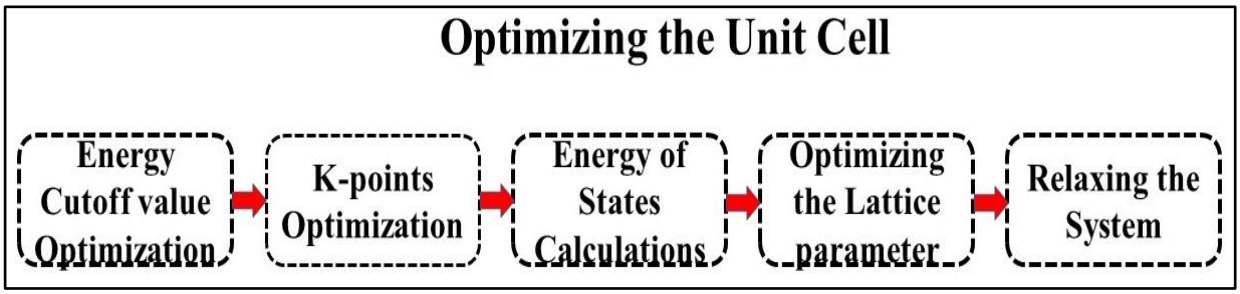

Fig. 5.1 : Flow diagram of Unit Cell Optimization.

The energy cutoff value for the Graphene unit cell was optimized to check the minimum energy corresponding cutoff value. Since the plane waves are the basis set i.e. combination of a set of function we use to define the wavefunctions, the more we include the better we can define the wave function. But including the higher energy planewaves will have minor improvements in our definition of the wave functions and will simultaneously increase the computational time and cost. Therefore, it is

important to check the energy cut off value before we venture into further calculations. A flow diagram depicting the steps performed in order to optimize the unit cell is given in Fig.5.1.

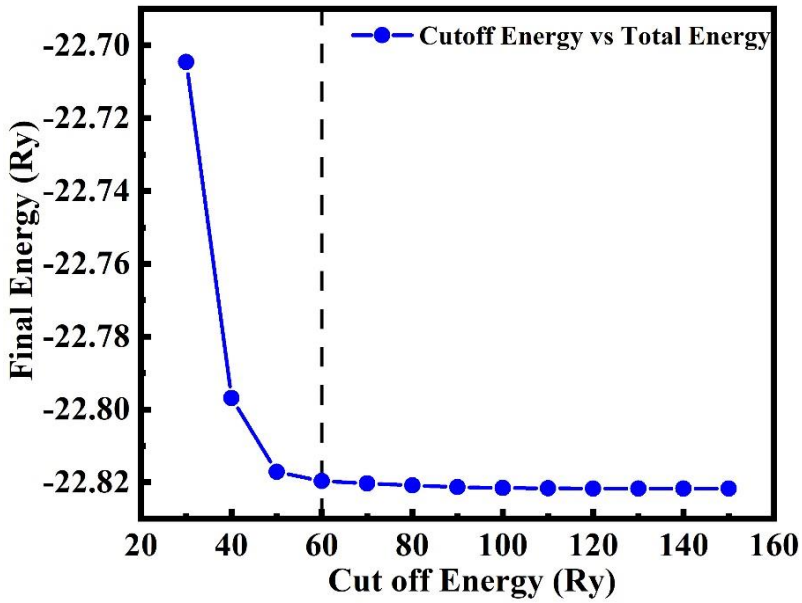

Fig. 5.2 : Final Energy Vs Energy Cutoff value.

From the above figure we find that the change in energy with respect to the energy cut off value becomes nearly constant from 60Ry. Therefore, for further calculations we use 60Ry as the energy cut off value. Similarly, K-points are also required to be optimized since it is practically impossible to calculate the electronic structure of an infinite system. For sampling of the Brillouin zone, the optimal number of k-points needs to be calculated in order to predict the electronic structure. Here as we are dealing with 2-D materials, we check the number of points in X and Y direction with respect to the minimum energy.

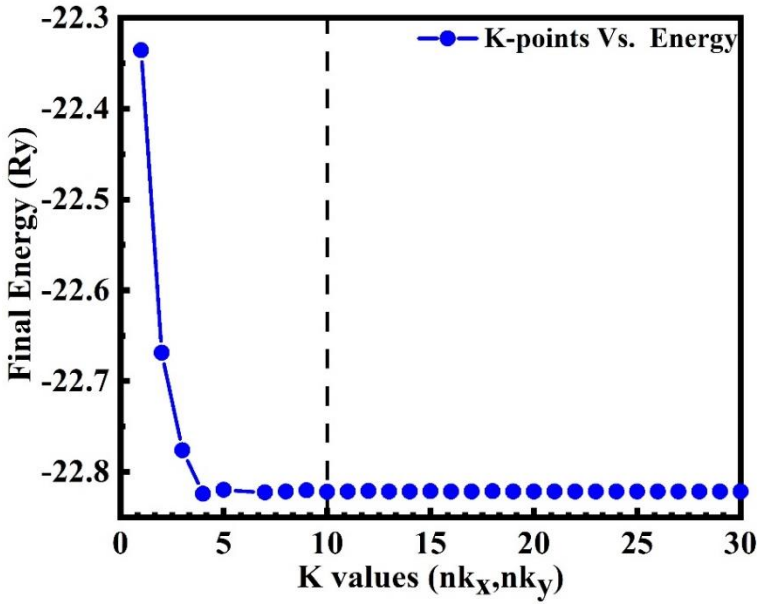

Fig. 5.3 : Final Energy Vs Number of K-points.

The number of K-points corresponding to the minimum energy was calculate to be 10 X 10 for the X and Y directions and since we are concerned with 2-D monolayer, we assume the number of K-points in the Z direction to be one. Therefore, the K-point grid was fixed as 10 X 10 X 1 for further calculations. Given the energy cut off value and the K-points, we optimized the lattice parameter corresponding to minimum energy and zero pressure.

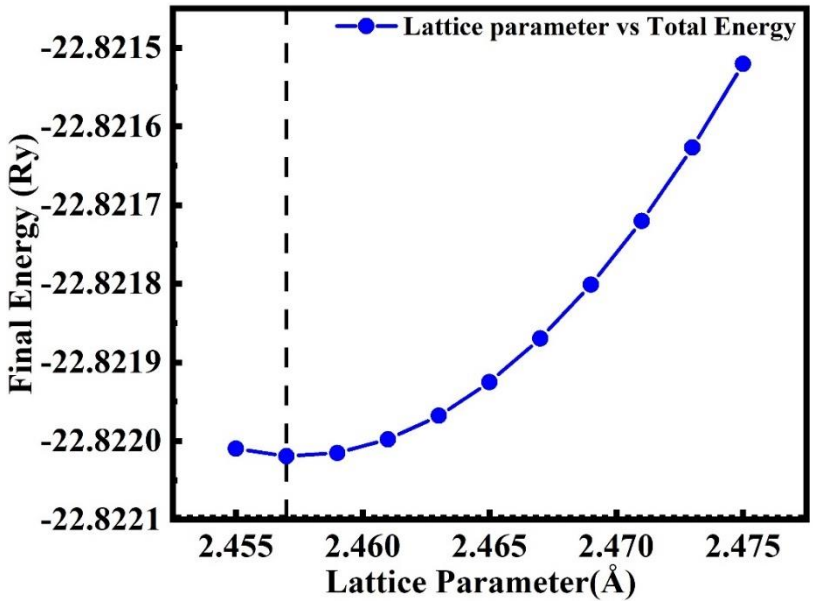

Fig. 5.4 : Final Energy Vs Lattice Parameter.

The lattice parameter was found out to be 2.457Å. With the given parameters, the unit cell was relaxed i.e. relaxing the cell parameter along with the atomic positions. The optimized unit cell was then used to draw a sheet of 4 X 4 Graphene sheet. The atomic positions of this sheet was then relaxed and obtaining the relaxed coordinates along with the total energy of the system. Thereafter, further calculations were performed in order to calculate the band structure, adsorption energy, DOS and PDOS. The flow diagram in Fig.5.5 shows the flow of calculations performed.

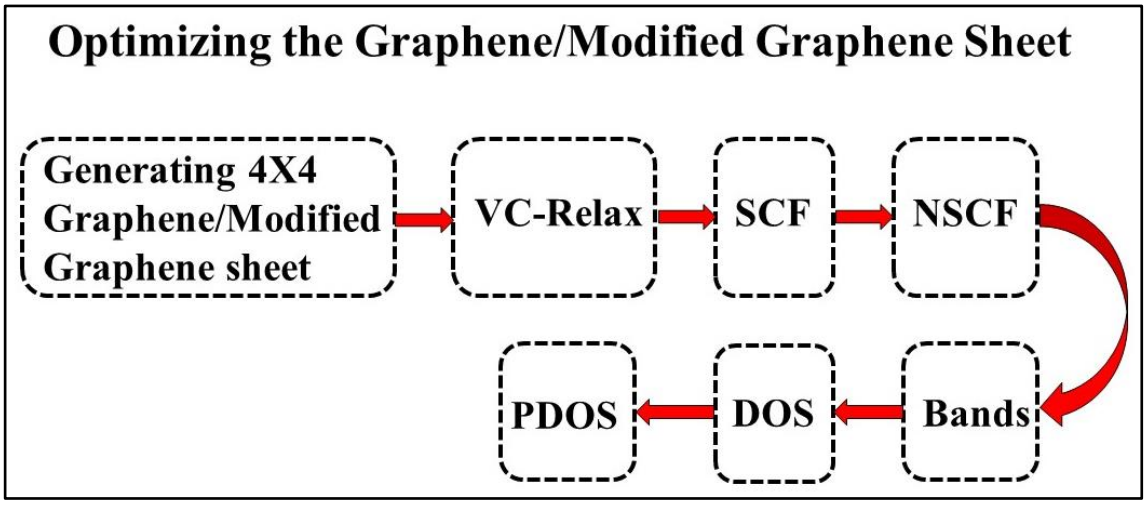

Fig. 5.5 : Flow Chart for calculations of the sheet.

The VC-Relax (VC- Variable Cell) functionality in the PlaneWave module implemented in the Quantum Espresso code, relaxes the cell parameters such as cell shape, angle along with the atomic coordinates. It also calculates the forces and the stress tensor. Now with the obtained optimized coordinates of the system, we perform the self-consistency test for the KS equation using the SCF (Self Consistent Field) functionality. The solution of the KS equation is carried out trying to minimize the charge density functional until the provided convergence limit is achieved. It also calculates the convergence with respect to the k-mesh points. Thus, with the help of SCF, we obtain the minimum energy that corresponds to the ground state of the system. However, in case of Band Structure calculation we require a denser k-points mesh and therefore NSCF or Non-Self Consistent Field calculation is required to be performed taking into consideration sampling of denser k-point mesh. After SCF and NSCF when we actually calculate the Energy Band profile, we provide actual values of the k-points preferably in the high symmetry k path in the Brillouin Zone.

Similar methodology was employed in order to optimize the modified Graphene sheet.

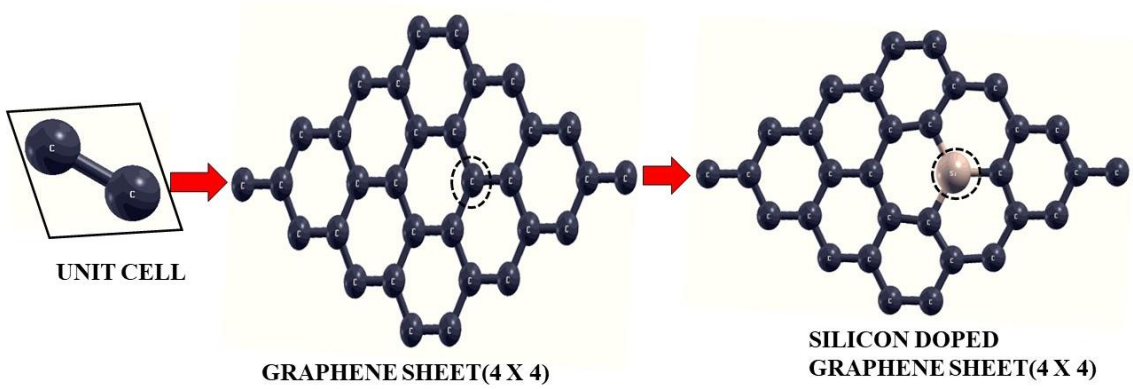

Fig. 5.6 : Schematic of graphene unit cell, pristine graphene sheet and doped graphene sheet.

For Valine Molecule, the coordinates were obtained from the Materials Project Database and relaxed. Thereafter, the calculations of the combined system i.e., Graphene/Modified Graphene Monolayer + Valine, was performed.

Summarizing the parameters used for calculations:

1) To fully converge the lattice parameters and the total energy of the systems, the energy cut off value for the charge density and plane wave basis set were taken as 60Ry and 600Ry.

2) For the unit cell as well as the supercell (4X 4), 10 X 10 X 1 K-point grids were used for reciprocal lattice integration calculations in the Monkhorst-pack scheme.

Structural optimization, adsorption energy and Density of States (DOS) calculations were performed in order to understand the interaction behaviour of valine amino acid with pristine graphene and Si-doped graphene. In order to accurately predict the interaction of nucleobases with nano-surface, the dispersion forces need to be taken into account. Grimme's dispersion correction is therefore been incorporated in the calculation to take into consideration the long range van dar Waals interaction between the surface the amino acid. Adsorption energy E_{ad} can thus be calculated from the equation given below:

$$E_{ad} = E_{\text{Graphene/Modified Graphene-Valine}} - (E_{\text{Graphene/Modified Graphene}} + E_{\text{Valine}})$$

$E_{\text{Graphene/Modified Graphene-Valine}}$ in the above equation represents the total energy of Valine adsorbed on the Graphene/Modified Graphene surface whereas, $E_{\text{Graphene/Modified Graphene}}$ and E_{Valine} are the total energies of the Graphene/Modified Garphene monolayer and that of Valine respectively.

5.2 Results and Discussion

5.2.1 Structural Properties

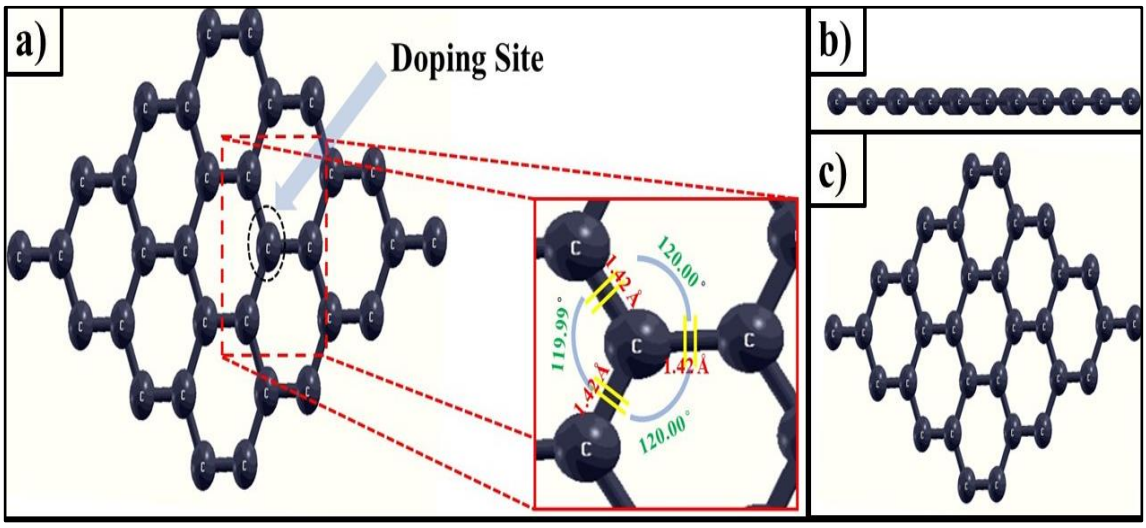

Fig. 5.7 : The optimized structure of pristine graphene sheet.

In order to calculate the structural properties of Pristine Graphene and Si-doped Graphene, we have first optimized the geometry and associated parameters of the unit cell of Graphene monolayer calculating it's lattice parameter and ground energy state. Thereafter, we have drawn a 4 X 4

Graphene sheet by periodically repeating the optimized unit cell and relaxed it's coordinates. This provided the optimized lattice parameters of the sheet along with the ground state energy of the system. The optimized structure is depicted in Fig. 5.7. Fig. 5.7 b) and c) shows the different views of the hexagonal structure : side view and top view respectively. In Fig. 5.7 a), we have represented the proposed site of introducing the dopant atom. For ease of understanding, we have named the doping site carbon as C^*. The C-C^* bond length is calculated to be 1.42 Å and the C-C^*-C bond angle is found out to be 120.00˚. For the purpose of modifying the Graphene sheet with Silicon as a dopant, we replace the C^* atom with a Silicon atom. The coordinates of the modified sheet was then relaxed and optimized giving the lattice parameters and the ground state energy.

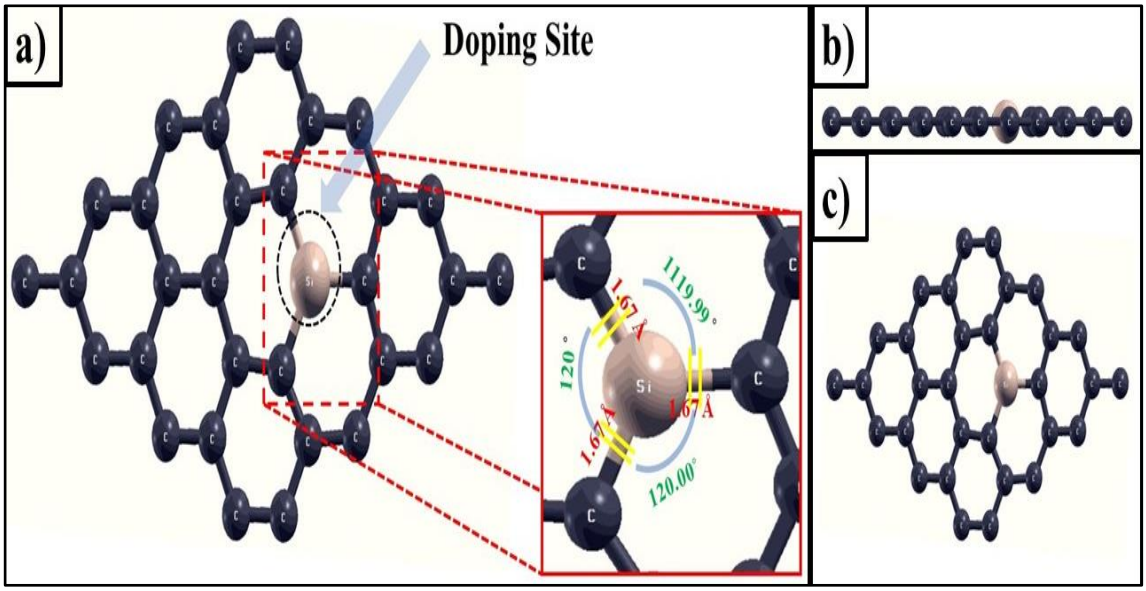

Fig.5.8: The optimized structure of Si-doped Graphene sheet.

In Si-doped structure, as we can see from Fig. 5.8, the C-Si bond length and the bond angle of C-Si-C was calculated to be 1.67Å and 119.99˚ respectively. From the calculated valve it is evident that Silicon atom on incorporation is causing distortion in the structure by pushing away it's adjacent carbon atoms and thus increasing the bond length. The bond angle however remains comparable with that of C-C^* in the pristine sheet. Calculated bond length and bond angles for graphene and Si-doped graphene are similar to the already reported values.[72] The bond angle and bond lengths are tabulated in Table 5.1

Table 5.1: Bond length and Bond angle of the optimized systems.

System	Bond Length(Å)	Bond Angle(˚)
pristine graphene	1.42 (C-C*)	120.00(C-C*-C)
Si-doped graphene	1.67 (C-Si)	119.99(C-Si-C)
pristine graphene + valine	1.42(C-C*)	120.02(C-C*)
Si-doped graphene + valine	1.73(C-Si)	108.07(C-Si-C)

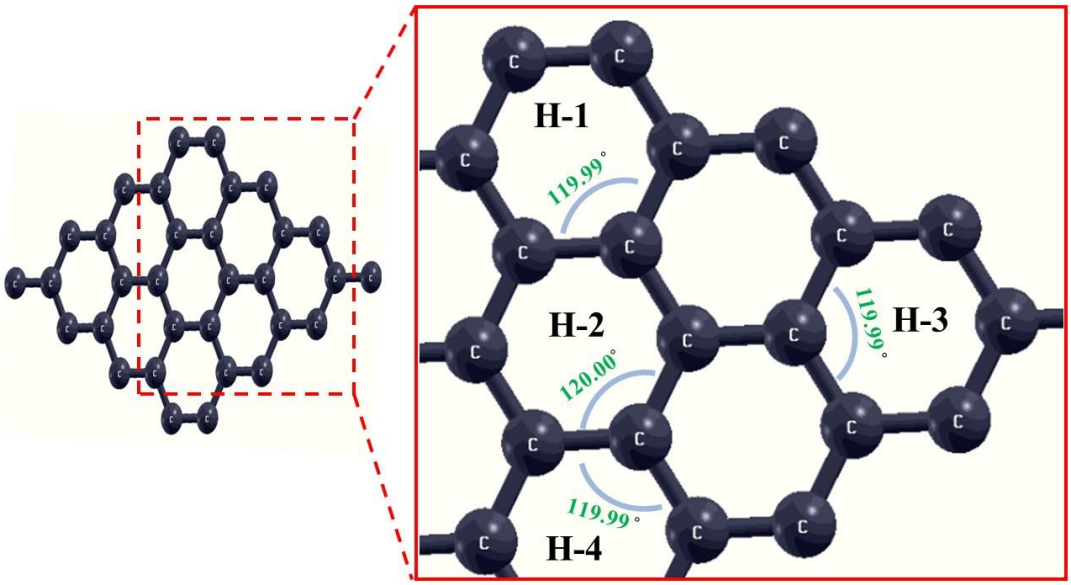

Fig. 5.9: The bond angles in the hexagonal rings around the doping site in pristine graphene.

The addition of the dopant atom results in the distortion of the hexagonal rings. It can be seen from Fig. 5.10 that due to the substitution, there has been a considerable change in the C-C-C bond angles in the hexagonal rings (see H1,H2,H3,H4 in Fig. 5.10) adjacent to the doping site. This distortion of the hexagonal rings from it's symmetry in the pristine form (see Fig. 5.9) can only be seen in the vicinity of the doping site while geometry of the rings away from the site continues to be in their pristine form. The bond length of C-C atoms in the rings adjacent to the doping site remains almost in line with that in pristine graphene.

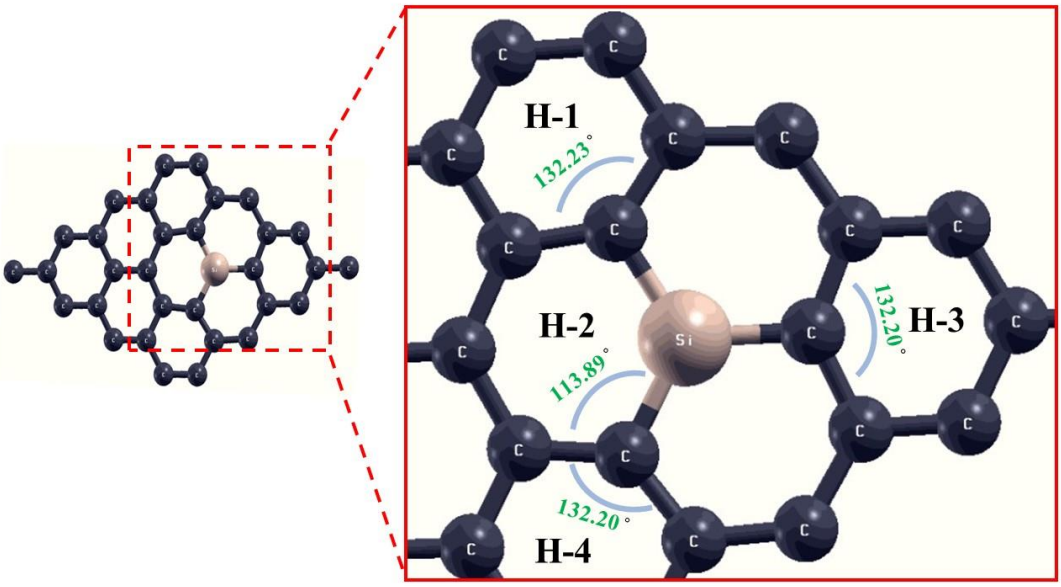

Fig. 5.10: The bond angle changes in the hexagonal rings around the doping site in Si-doped graphene.

Pristine Graphene monolayer has a planar geometry and is formed due to very strong σ bonding of the 2s, $2p_x$ and $2p_y$ orbitals and weak Π bonding of the $2p_z$ orbitals which is perpendicular to the planar surface. As we dope or rather substitute a carbon atom in the pristine structure with a Silicon atom, the planar structure remains constant but we see some distortion and lengthening of the C-Si bonds. The C-C* bond length in case of pristine happens to less than that of C-Si in the doped system. This is possibly due to the participation of some of the carbon electrons in multi-orbital hybridization of Si-C bond resulting weakening of the C-C bond. Moreover, the Si-doped graphene sheet remaining planar signifies strong quasi- σ bonds as a result of sp^2-sp^2 multiple orbital hybridization. Given that the calculated bond length and bond angles of the pristine and doped system are strongly comparable with that mentioned in published literatures.[72]

The lattice parameters of the graphene and Si-doped sheets alone as well in combined state were also calculated to further investigate the effect of doping and adsorption on the lattice parameters. The calculated values are tabulated in Table 5.2. It is evident that due to the incorporation of Si atom, the lattice parameters have subsequently been increased.

Table 5.2: Lattice parameters, D, E_g and E_F of the optimized systems.

System	Lattice Parameter (Å)	Distance between monolayer and molecule(D)(Å)	E_g (Energy Band Gap)(eV)	E_F (Fermi Energy) (eV)
pristine graphene	9.84	--	--	-2.53
Si-doped graphene	10.02	--	0.22	-2.53
pristine graphene + valine	9.83	2.70	--	-2.06
Si-doped graphene + valine	9.93	2.27	--	-1.99

For investigation of the adsorption behaviour of the surfaces with Valine, we had obtained the atomic coordinates of the molecule from PubChem Database[100] and relaxed them to optimize the structure with respect to the cell parameter of our base system. The optimized structure of valine molecule is shown in Fig. 5.11

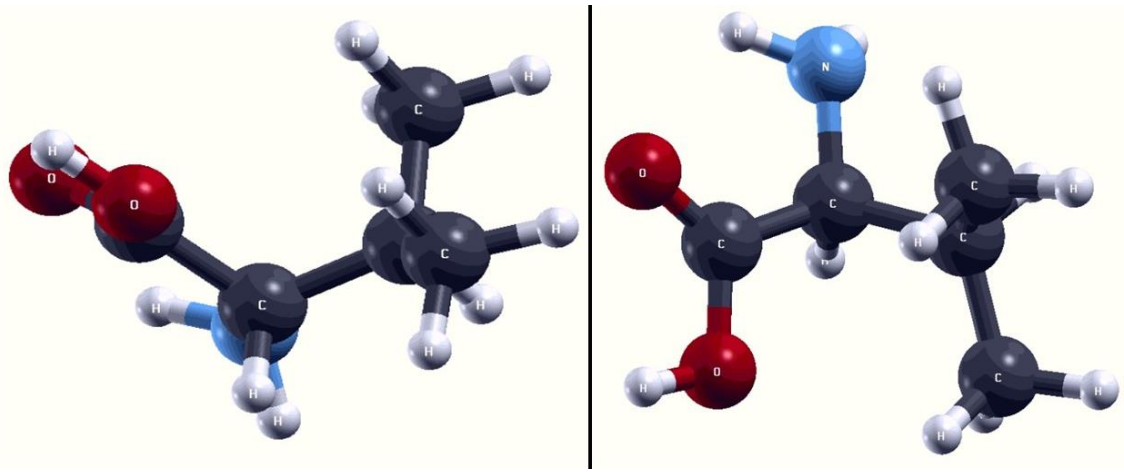

Fig.5.11: The optimized structure of Valine molecule in different orientations.

5.2.2 Electronic Properties

Fig. 5.12: The doping site atom(C^*) and the adjacent atom(C) depicted on the graphene sheet.

In order to understand the electronic properties, it is essential to calculate and study the band structure diagrams of the structures alone as well as when in combination with the molecule. The band structure of all the systems are calculated by sampling the k-points in the high symmetry direction of the Brillouin zone along the **Γ-M-K-Γ** k-path. For calculating the electronic properties, we take into consideration of doping site carbon atom(C^*) and the adjacent carbon atom(C) for pristine system and for doped system we consider the adjacent carbon atom (C) and Si in the doping site. A schematic of the same is represented in Fig. 5.12. The calculated band structures of the systems can be seen in Fig. 5.13 and Fig. 5.14. In Fig. 5.13, the band structure of pristine graphene is shown along with the Density of States(DOS) and the Partial Density of States(PDOS).

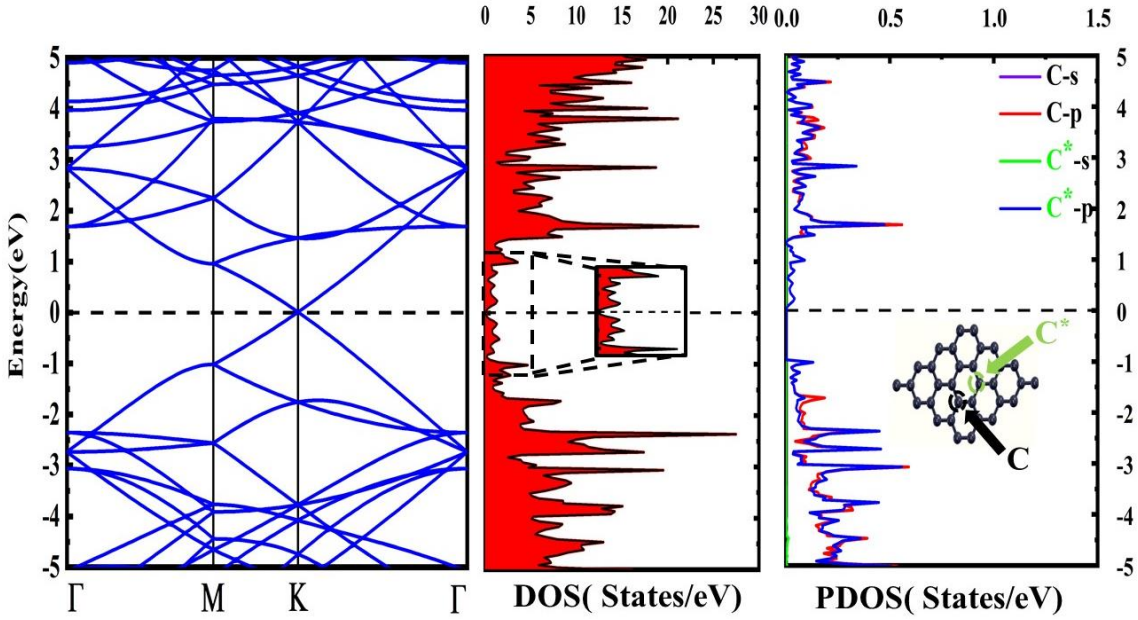

Fig. 5.13: The band structure, DOS and PDOS of pristine graphene.

The band diagram of pristine graphene depicts the asymmetry of the occupied valence bands about the unoccupied conduction bands. This is mainly due to the multi orbital σ bonds. The DOS seize to exist at the Fermi level and therefore pristine graphene is termed as zero-gap semiconductor. Formation of the isotropic Dirac cone takes place at low energy. The formation of the Dirac cone is due to the hexagonal symmetry of pristine graphene.

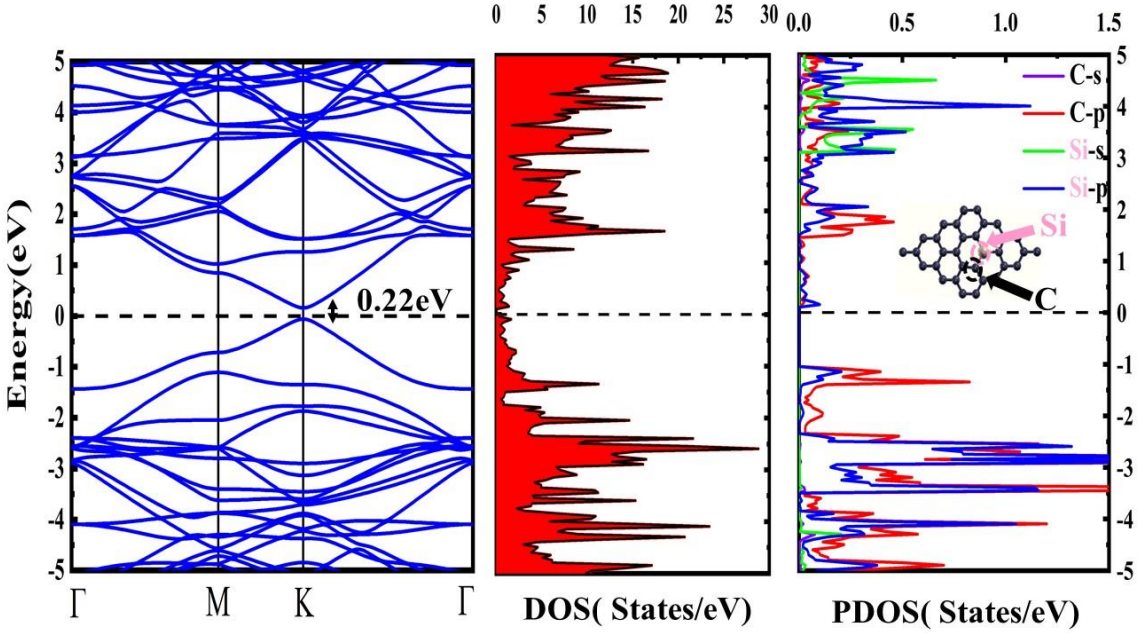

Fig. 5.14: The band structure, DOS and PDOS of Si-doped graphene.

However when the pristine structure is doped with Silicon, there is a separation of the conduction and valence band Dirac points (see Fig. 5.14). The separation was calculated to be ~0.22 eV. Though

while comparing the Fermi energy of these two systems we didn't find much difference and they were almost comparable. The DOS of Si-doped Graphene shows presence of electronic states close to the Fermi level on either side of conduction and valence band.

From the PDOS (Fig. 5.15)) calculated, it can be conferred that in case of pristine graphene, that C^* atom's p-orbital along with the p-orbital of the adjacent carbon atom have considerably greater contribution to the DOS on either side of the Fermi Level. Among the components of the p orbitals of C^* and C atoms, it is the p_x orbitals of both the atoms that show greater contribution to the total DOS near the Fermi level.

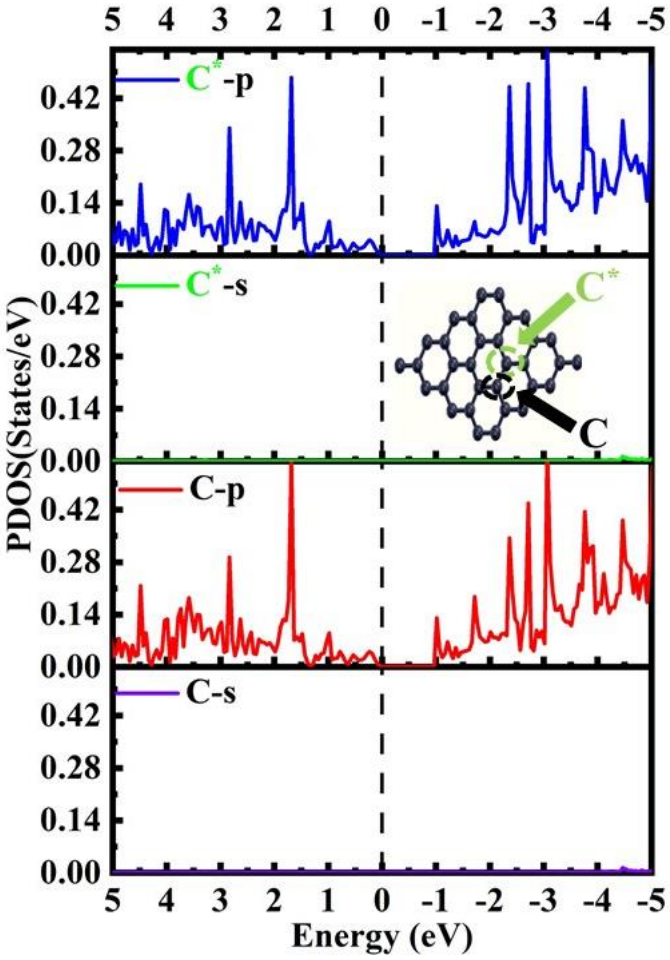

Fig.5.15: Partial DOS of pristine graphene.

In case of Silicon doped graphene (Fig. 5.16), the s and p orbitals of Si atom along with the p-orbital of the adjacent carbon atom shows significant contribution to the DOS around E_F. Here, close to the E_F on the conduction side we see greater contribution of the p-orbital and as we move further away from the Fermi level on both the sides, the intensity of the contribution increases.

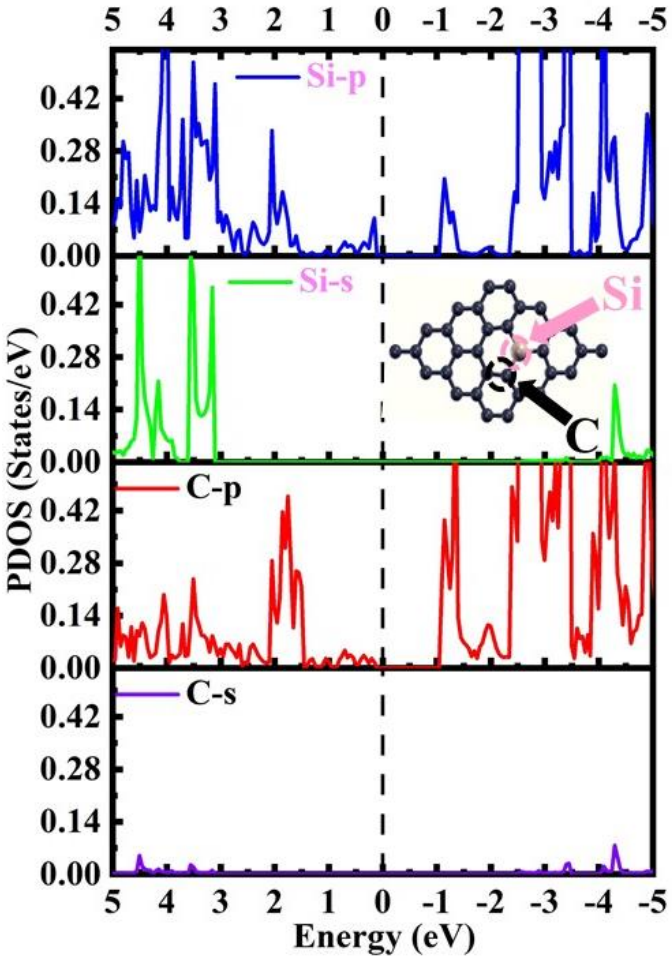

Fig.5.16: Partial DOS of Si-doped graphene.

The lowdin's charge calculation was performed in order to see whether the incorporation of Si-atom resulted in any charge transfer to the surrounding carbon atoms. It was found that due to Si-atom doping, there was a +2.78e gain in the Lowdin's charge of the monolayer. Therefore, it is evident that Si-atom transfers charge to it's adjacent carbon atoms.

5.2.3 Adsorption

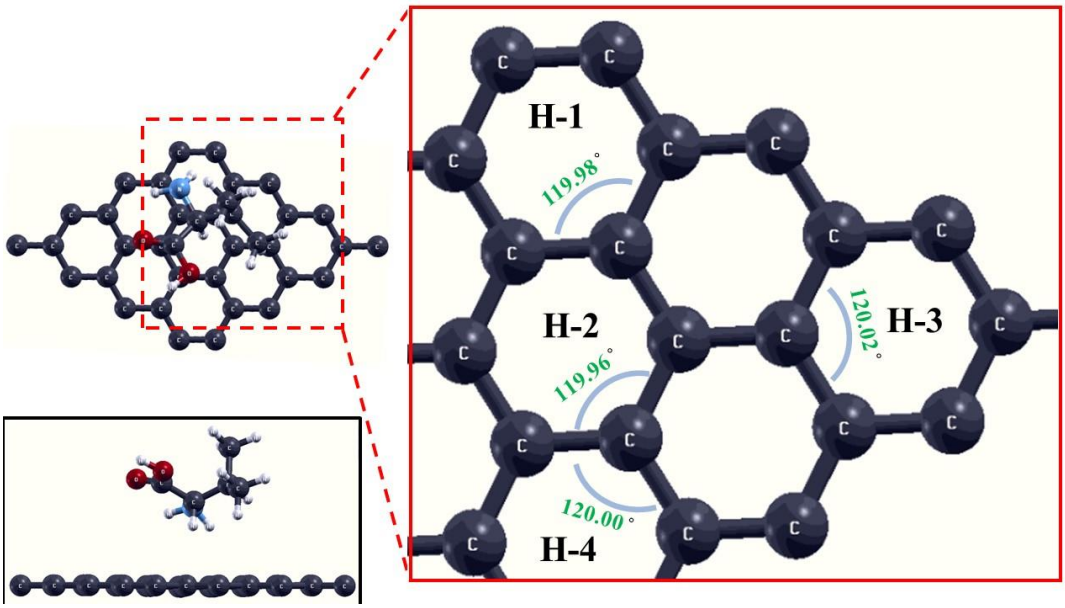

Fig.5.17: The optimized structure of valine adsorbed on pristine graphene.

For adsorption study, we had placed the Valine molecule over the graphene/ modified graphene sheet keeping a considerable distance between them and then relaxed the system. The molecule was preferably placed over the doping site to investigate the contribution of the doping to the interaction of the sheet with the molecule. After relaxing the system, the ground state energy of the systems viz. Pristine Graphene/Valine(GV) and Si-doped Graphene/Valine(SGV) were calculated. Dispersion correction was included in this study to take into consideration the long range van dar Waals interaction. We did the calculations in the framework of DFT-D2 using Grimme's Dispersion Correction, taking into consideration the dispersive forces.

When Valine interacts with the pristine graphene and Si-doped graphene represented by the GV and SGV systems respectively (see Fig. 5.17 and Fig. 5.18), it was found that the C-C* bond length in case of graphene sheet remained almost unchanged whereas the C-Si bond length in Si-doped graphene sheet was further stretched to 1.73Å.

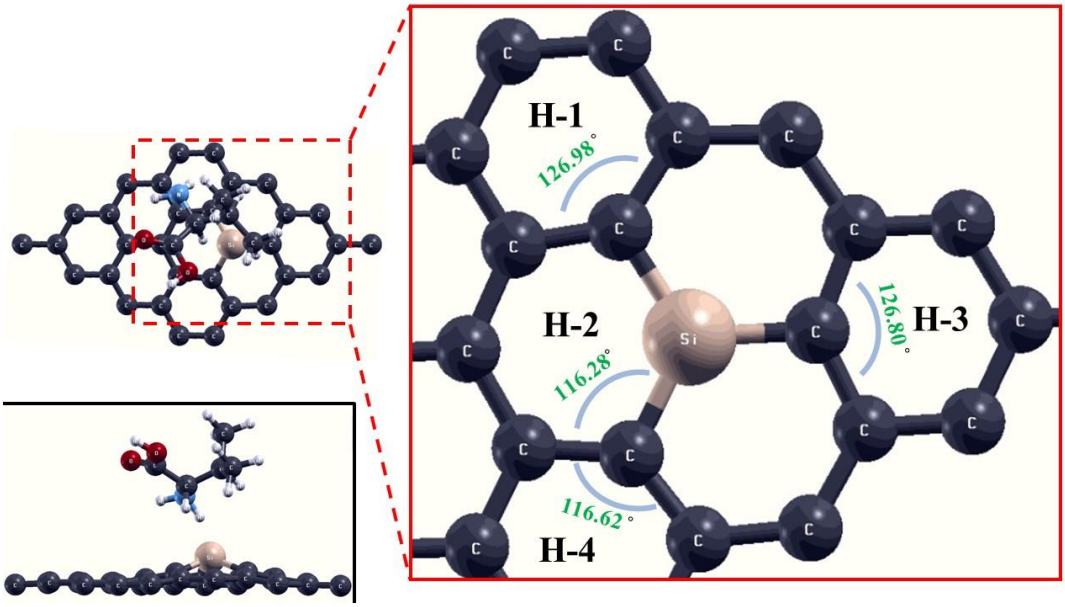

Fig.5.18: The optimized structure of valine adsorbed on Si-doped graphene.

Though the graphene sheet continued to be planar in geometry(see Fig.5.19), the Si-doped one showed stretching in the Z-axis for the Si atom. The Si-atom was raised to a height of 1.11 Å with respect to the planar carbon atoms due to interactions with Valine molecule(see Fig. 5.20). The stretching of the dopant atom along the Z direction possibly contributes to the increase in C-Si bond length. Due to stretching in the Z-direction of the Si atom, the distortion of the adjacent hexagonal rings was reduced as can be seen in Fig.5.18 but pristine conditions were not achieved.

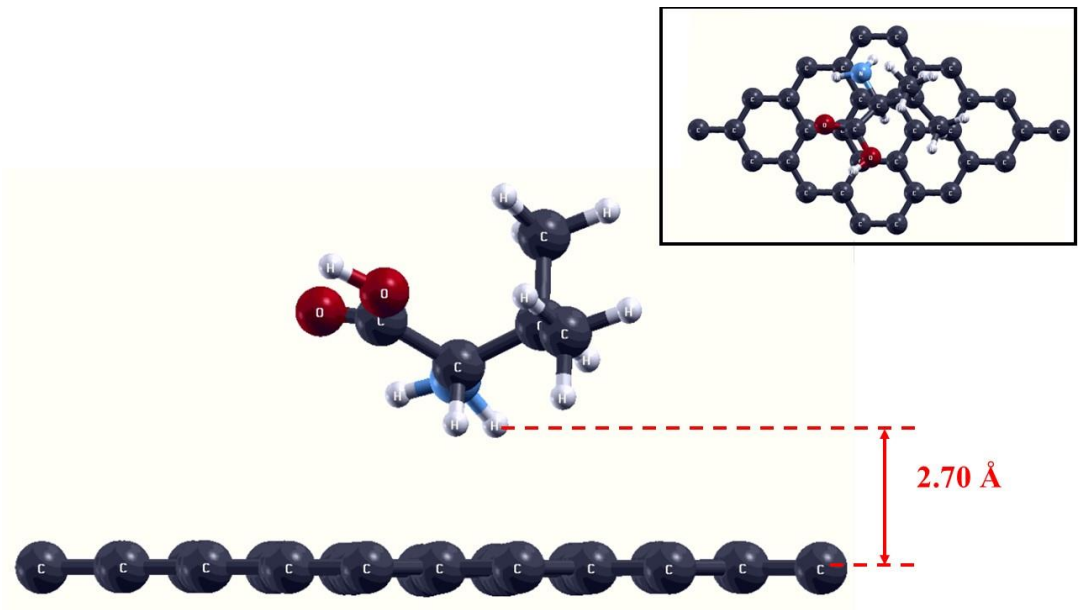

Fig. 5.19 : The distance between the molecule and pristine graphene sheet.

The height of the molecule above the sheets were calculated to be 2.70 Å and 2.27Å for GV and SGV systems respectively. The height was calculated considering the distance between Si atom and a hydrogen atom in the -NH_2 group present in Valine in the case of SGV system and for GV system it was calculated considering the planar carbon atoms and the hydrogen atom of amine group in Valine.

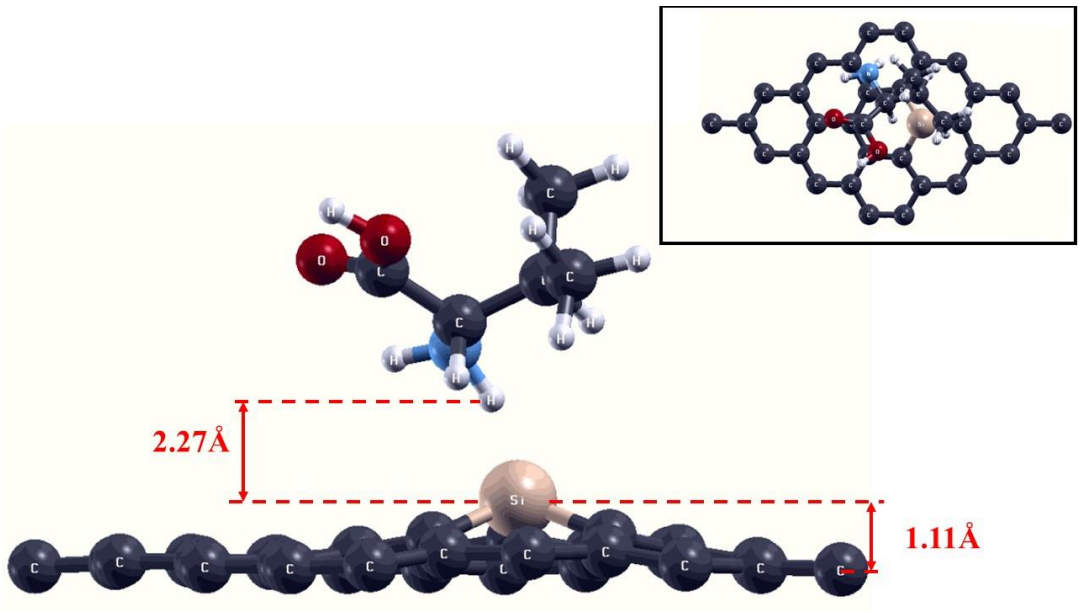

Fig. 5.20: The distance between the molecule Si-doped graphene sheet.

It can be commented that the possible mode of interaction of two functional group containing valine with the monolayer is via the -NH_2 group. In available literatures, it is mentioned that the interaction of monolayers with functional groups containing amino acids such as cysteine takes place via a preferred mode i.e., through which group the molecule will be interacting with the monolayers in case there are more than one.[101]

Given the range of the distances between the surface and the molecule, it is understood that the type of adsorption is physisorption or that the molecule is physically adsorbed on the surface. The adsorption energies calculated for Valine on Graphene and Si-doped Graphene are -0.41eV and -0.65eV respectively. Thus, it can be seen that Silicon doping has considerably increased the adsorption energy in comparison to pristine graphene.

The adsorption energy(E_{ads}) of Valine on pristine graphene is comparable with that mentioned by Petroshenko *et al.*in which the adsorption energy is calculated to be -0.49 eV. The adsorption energy of N-doped Graphene in the aforementioned literature is in the range -0.65eV to -0.82eV. The calculations were also done in the framework of DFT-D2 using Grimme's dispersion correction.

Slight change in the value of E_{ads} for valine on pristine graphene calculated here to that reported by

Petrochenko *et al* is possibly due to the fact that in this study we have performed the calculations for the graphene sheet consisting of 32 carbon atoms whereas they considered 48 carbon atoms.

Also, they had saturated the dangling bonds of the monolayer with H atoms. Therefore, given the of the adsorption value of valine adsorption on N-doped Graphene, it can commented that the adsorption energy for Si-doped graphene is also in range with that of it's N-doped counterpart. The energy calculated in this work shows an increase in the adsorption energy by ~60% for Si-doped over Pristine Graphene whereas for N-doped is reported to be ~65%.[70]

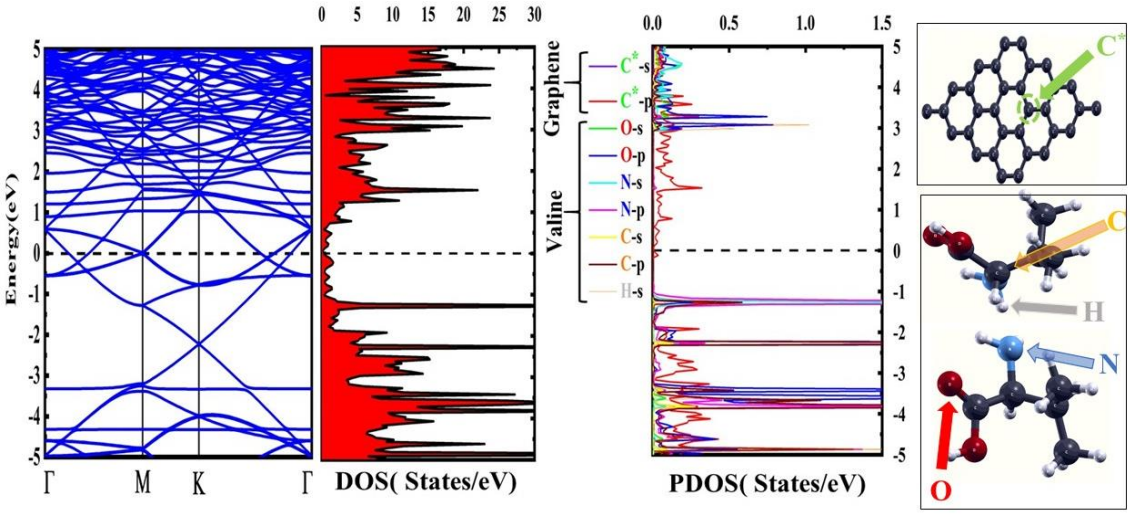

Fig. 5.21 : Band Structure, DOS and PDOS of pristine graphene + valine combined system.

In order to further investigate the nature of interaction of the adsorbate with the adsorbent, we have calculated the band structure, Density of States(DOS) and Partial Density o States(PDOS) of the combined systems viz. GV and SGV. With respect to pristine graphene, in case of GV we see an increase in energy bands near the Fermi Level which is evident from the Band Diagram as well as the DOS(see Fig.5.21). These extra occupied states in the band energy profile are credited to the molecular energy levels of Valine. The p orbital contribution of the C^* atom to the DOS remains almost unchanged in case of GV with respect to the pristine one. Apart from the contribution of C^* atom, the DOS depicts significant contribution from the N,C,H and O atoms present in the molecule. Since it is already mentioned that amino acids containing functional groups tend to interact with adsorbate substrate through any of the preferred groups, we have calculated the DOS and PDOS taking into consideration the following:

1) N atom of the $-NH_2$ group and O atom of the -COOH group has been considered to evaluate their role in adsorption.
2) H atom of the $-NH_2$ and C atom attached to the amine group has been considered since the functional group closest to the substrate surface is the $-NH_2$ group.

Therefore, the contribution of the aforementioned atoms of the molecules in the DOS and PDOS could help us to comment better on the participation of the functional groups.

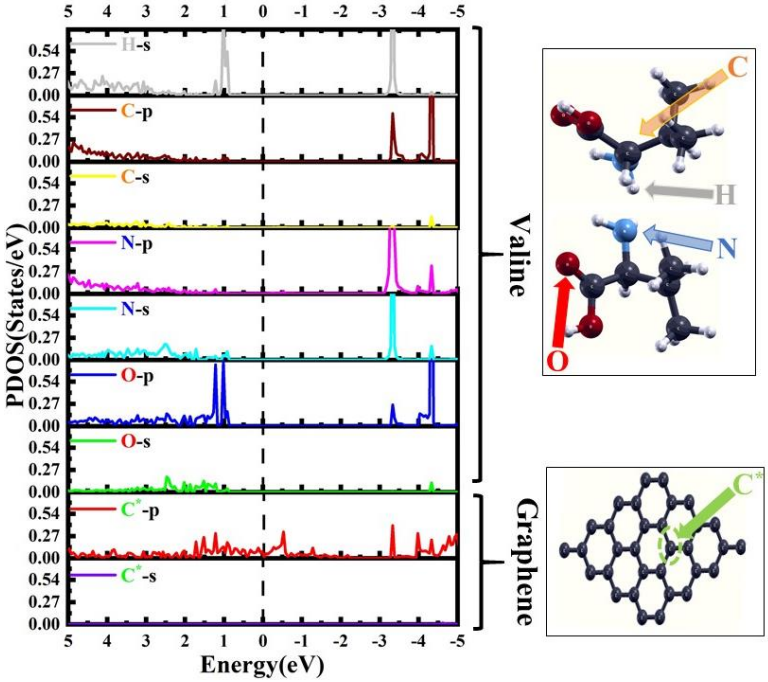

Fig. 5.22 : Partial DOS of valine adsorption on pristine graphene showing the effective contribution of the orbitals to the DOS.

In Fig. 5.22, we can see the contribution of the orbitals in total Density of States. The contributing orbitals of Valine molecule happens to be that of N, C and O atoms. Near the Fermi Level on the valence side, s and p orbitals of nitrogen atom in the amine group depict enhanced intensities. All the 3 p-orbitals viz. p_x,p_y and p_z of the N atoms have comparable contribution. Also, the H atom of the amine group is seen to actively participate in the interaction. Thus, the interaction and thereafter the adsorption of the amino acid on the graphene surface can be attributed to the impact of interaction between the -NH_2 group of the molecule and the C^* atom of the monolayer.

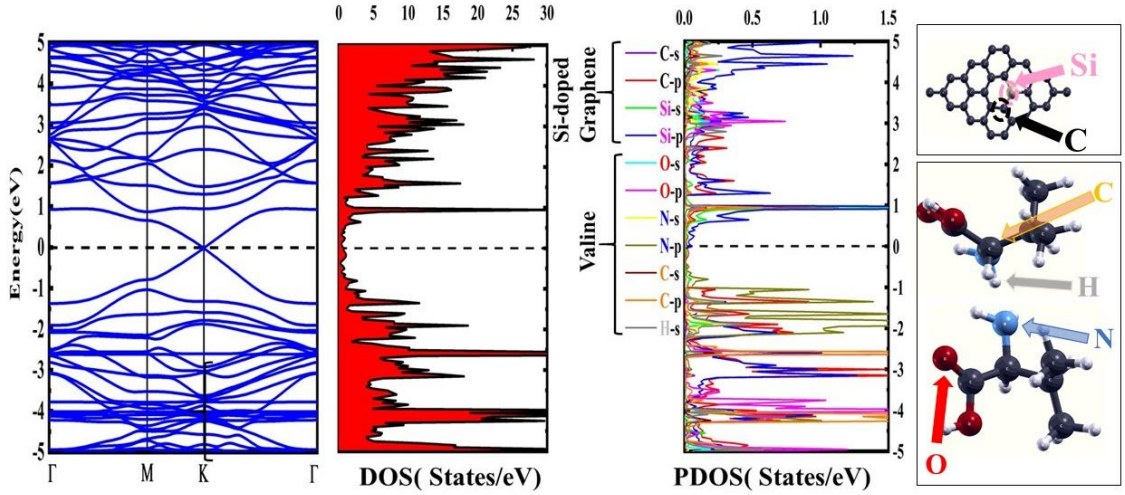

Fig. 5.23: Band Structure, DOS and PDOS of Si-doped graphene + valine combined system.

Similar to that of adsorption on pristine graphene, in SGV system, we find a significant increase in the number of bands in the Energy band profile(see Fig. 5.23). Occupied states exist at the Fermi level and is due to the s orbital contribution of the Si of the surface along with the p orbitals of Si, C of the substrate surface and that of N in valine. The same orbitals are found to have increased intensities around the Fermi level and thus increasing the DOS around it.

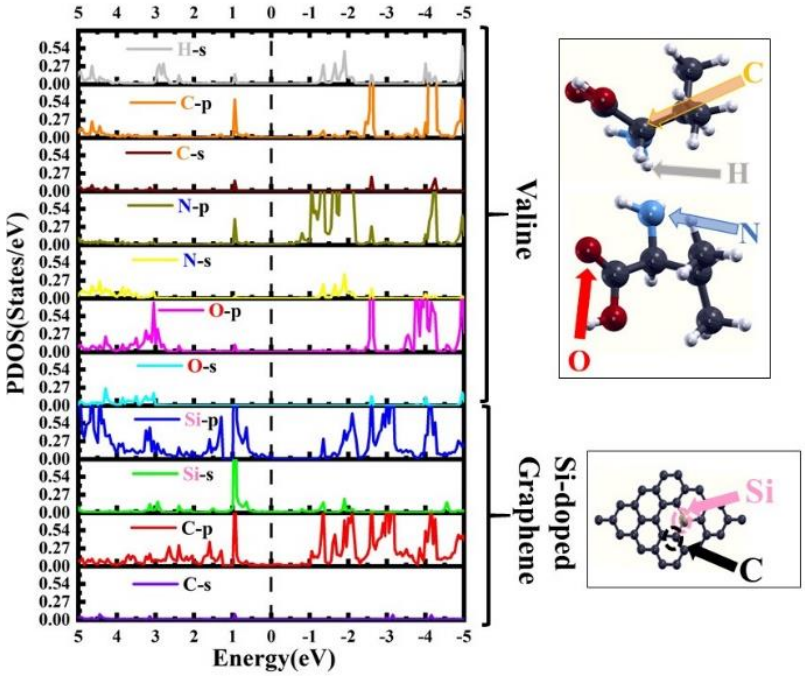

Fig. 5.24: Band Structure, DOS and PDOS of Si-doped graphene + valine combined system.

Again it can be inferred that the interaction of the molecule with the surface is mainly via the Silicon and Carbon of the doped surface and the N of the amine group present in valine. PDOS in Fig. 5.24 further establishes the relation between the interacting atoms.

Around E_F the occupied states are mainly due to the p orbitals of the dopant atom on the surface and N atom in the molecule. All the 3 p orbitals of both the atoms have occupied states around E_F. Thus, here also we can say that the adsorption is largely due to the interaction Si and N orbitals. Hydrogen is also seen to contribute to the DOS as well.

From the above analysis, it can be firmly said that in the mentioned orientation, the preferred mode of interaction of the amino acid molecule with the surface is via the $-NH_2$ functional group. As Si atom when incorporated in the base substrate of pristine graphene it transfers charge to the sheet, it tends to be positively polarized given that the surrounding carbon atoms are highly electronegative. This positively polarized part of the substrate possibly interacts with the negatively polarized Nitrogen in the $-NH_2$ group whereas it is possibly repealed by the positively polarized H atom in the amine group. The lack of this polarization in the pristine sheet also contributes to the fact that it has lower interaction energy.[73]

The lowdin's charge analysis for the adsorption was also calculated which showed a low transfer of charge from the molecule to the surface for both the systems. In the course of the interaction, Valine transferred 0.25e and 0.19e to the pristine and doped surface respectively. Since the charge transfer is almost comparable it cannot aptly justify the difference in E_{ads} for the studied surfaces. Therefore, the possible justification of the increase in E_{ads} for valine on Si-doped graphene in comparison Pristine Graphene can be drawn from the analysis of their respective Band diagrams, DOS and PDOS. The existence of densely occupied orbitals of Si atom near the E_F in comparison to that of C^* atom plays a significant role in interaction energy.

5.2.4 Recovery Time

The recovery time calculation of pristine and Si-doped graphene was done in order to check the feasibility of their use as a carrier of Valine and their reusability. In experimental set-up, the recovery time can be calculated by heating the substrate, but in case of computational approach, in order to estimate the recovery time, the following expression is used:

$$\tau = \upsilon^{-1} e^{\frac{-E_{ads}}{KT}} \quad (5.1)$$

Where υ is the attempt frequency, T is the temperature and K is the Boltzmann constant. For the purpose of our calculations, we have considered the attempt frequency to be 10^{12} s^{-1}[102]. The room

temperature(298K) recovery time for graphene and Si-doped graphene for Valine was calculated to be 0.0073ms and 92ms respectively. These values show that the adsorption of valine on graphene is weak with respect to that on Si-doped graphene and thus, it can be removed very fast from the surface.

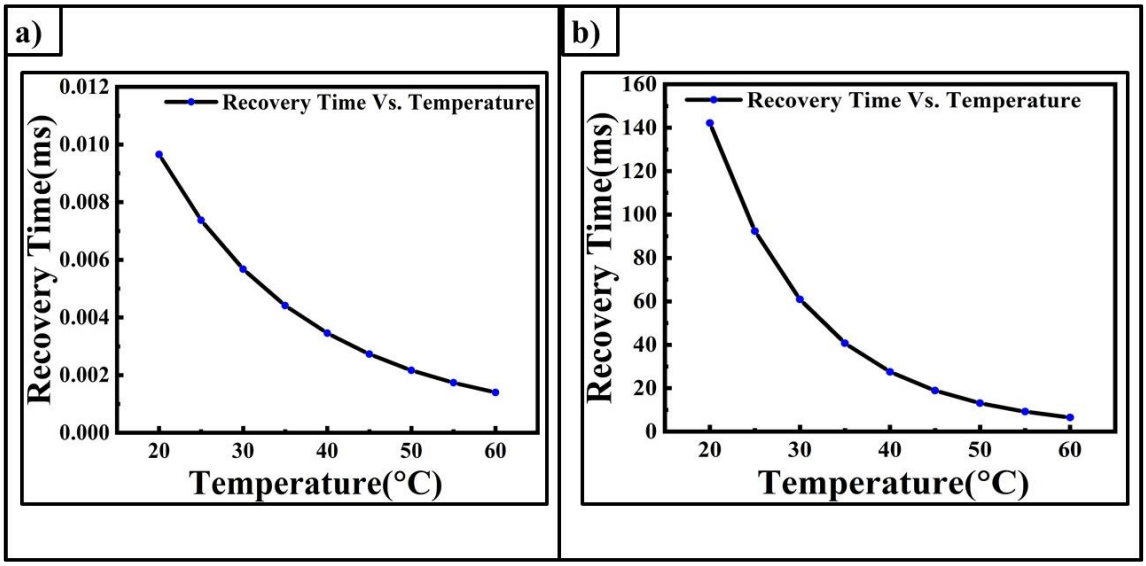

Fig. 5.25: Recovery Time of Valine adsorbed on a) pristine graphene and b) Si-doped graphene with increase in Temperature.

The recovery time for both the systems were calculated in the temperature range 20℃-60℃ to establish the relation between their recovery time and temperature. Fig. 2.25 shows the Recovery Time Vs. Temperature profile for both the systems. For both the systems the recovery time decreased with increase in temperature. This can be contributed to the fact that as we increase the temperature, we provide energy to the system and increase their lattice vibrations and thus, the molecules get de-adsorbed faster. Therefore, it can be concluded from the above values that with the enhanced adsorption energy and ultrafast recovery time, Si-doped Graphene has greater potential to be used as a re-usable biosensor for Valine in comparison to pristine graphene.

Chapter 6 : Summary and Future Work

In this report, we start off giving a brief introduction on Graphene: it's history, applications of Pristine Graphene, various modified graphene and their applications; then moving to Bio-conjugate systems. The utilization of unique and tailor made properties of Graphene/ Modified Graphene in Biomedical research is studied in details. Theoretical study on the interaction mechanisms for various biomolecules with 2-D materials is thoroughly explained. Thereafter, the report briefed on the biological importance of Amino Acids and in particular Valine. Thus, setting the stage for the present work. A brief introduction of the theoretical methodology which will be employed for the research work is mentioned. With this fundamental understanding of the background and the methodology, we try to understand the mechanism of interaction between Valine and Doped Graphene(Si-doped). Using Quantum Espresso code, within the framework of GGA-PBE along with dispersion correction(DFT-D2), we performed all the calculations. Optimizing the unit cell of the graphene sheet, we obtained an cut off energy value of 60Ry corresponding to the minimum energy. Similarly, the number of k-points and lattice parameters were optimized giving values of 10 X 10 and 2.465 Bohr respectively. The structure of the pristine and doped graphene sheets were optimized. The bond angle and bond lengths calculated were comparable with earlier reported values. Si atom doping the pristine substrate resulted in a very small band gap of ~ 0.22 eV. The charge transfer calculation showed the increase in charge of the pristine sheet when Si atom is doped. Adsorption studies of the substrates showed enhanced adsorption energies of vaine on Si-doped surface in comparison to that of the pristine form. For doped surface the energy value was calculated to be 0.65eV whereas for pristine it was 0.41eV. The possible reason for the greater interaction is due to the difference in nature of polarization. Si atom being positively polarized interacts strongly with the negatively polarized N atom of the molecule. Recovery time calculations of doped surface showed ultrafast recovery time i.e., 92ms at room temperature and that of pristine surface was almost negligible asserting low adsorption energies. The conclusion drawn from this work is that Si-doped Graphene can be used as a biosensor for Valine over Graphene. Also the fact that Si-doped Graphene has already been synthesized experimentally, the reported values in this work can help experimentalist to further investigate this interaction experimentally.

References :

[1] H. Cheun Lee, Wei-Wen Liu, Siang-Piao Chai, Abdul Rahman Mohamed, Azizan Aziz, Cheng-Seong Khe, N. M. S. Hidayah and U. Hashim ," Review of the synthesis, transfer, characterization and growth mechanisms of single and multilayer graphene", RSC Advances, Issue 26, 2017.

[2] Matthew J. Allen, Vincent C. Tung and Richard B. Kaner, " Honeycomb Carbon: A Review of Graphene", Chem. Rev. 2010, 110, 132–145.

[3] "Graphite intercalation compounds and applications"; Endo, M., Ed.; Oxford University Press: 2003.

[4] Shaffault, P. J. J. Prakt., "Graphite intercalation compounds", Chem. 1841, 21, 155.

[5] L. M. Viculis, J. J. Mack, R. B. Kaner, "A Chemical Route to Carbon Nanoscrolls" Science 2003, 299, 1361.

[6] L. M. Viculis, J. J. Mack, O. M. Mayer, H. T. Hahn, R. B. Kaner, "Intercalation and exfoliation routes to graphite nanoplatelets", J. Mater. Chem. 2005, 15, 974.

[7] X. L. Li, X. R. Wang, L. Zhang, S. W. Lee, H. Dai, "Chemically derived, ultrasmooth graphene nanoribbon semiconductors ", J. Science 2008, 319, 1229.

[8] X. K. Lu, M. F. Yu, H. Huang, R. S. Ruoff, "Tailoring graphite with the goal of achieving single sheets", Nanotechnology 1999, 10, 269.

[9] K. S. Novoselov, A. K. Geim, S.V. Morozov, D. Jiang, Y. Zhang, S. V. Dubonos, I. V. Grigorieva, A. A. Firsov, "Electric Field Effect in Atomically Thin Carbon Films ", Science 2004, 306, 666.

[10] Y. B. Zhang, J. P. Small, W. V. Pontius, P. Kim, "Fabrication and electric-field-dependent transport measurements of mesoscopic graphite devices", Appl. Phys. Lett. 2005, 86, 073104-1.

[11] W. Choi, I. Lahiri, R. Seelaboyina and Yong Soo Kang, " Synthesis of Graphene and Its Applications: A Review", Critical Reviews in Solid State and Materials Sciences, 35:52–71, 2010.

[12] J. Hass, W. A. de Heer, and E. H. Conrad, "The growth and morphology of epitaxial multilayer

graphene", J. Phys. Cond. Matter, 20, 323202, 2008.

[13] C. N. R. Rao, K. Biswas, K. S. Subramanyam, and A. Govindaraj, "Graphene, the new nanocarbon", J. Mater. Chem., 19, 2457, 2009.

[14] A. H. Castro Neto, F. Guinea, N. M. R. Peres, K. S. Novoselov,and A. K. Geim, "The electronic properties of graphene", Rev. Mod. Phys., 81, 109, 2009.

[15] K. S. Novoselov, A. K. Geim, S. V. Morozov, D. Jiang, M. I. Katsnelson, I. V. Grigorieva, S. V. Dubonos, and A. A. Firsov, "Two-dimensional gas of massless Dirac fermions in graphene", Nature, 438, 197, 2005.

[16] K. S. Novoselov, Z. Jiang,Y. Zhang, S.V. Morozov, H. L. Stormer, U. Zeitler, J. C. Maan, et al., "Room-temperature quantum Hall effect in graphene" , Science, 315, 1379 , 2007.

[17] F. Schedin, A. K. Geim, S. V. Morozov, E. W. Hill, P. Blake, M. I. Katsnelson, and K. S. Novoselov, "Detection of individual gas molecules adsorbed on graphene", Nature Materials, 6, 652, 2007.

[18]. J. S. Bunch, A. M. van der Zande, S. S. Verbridge, I. W. Frank, D. M. Tanenbaum, J. M. Parpia, H. G. Craighead, and P. L. McEuen, "Electromechanical resonators from graphene sheets", Science, 315, 490 , 2007.

[19]. C. Lee, X. Wei, J. W. Kysar, and J. Hone, "Measurement of the elastic properties and intrinsic strength of monolayer graphene", Science, 321, 385, 2008.

[20] H. Chen, M. B.M¨uller, K. J. Gilmore, G. G. Wallace, and D. Li, "Mechanically strong electrically conductive and biocompatible graphene paper", Adv. Materials, 20, 3557, 2008.

[21] K. S. Novoselov, E. McCann, S. V. Morozov, V. I. Fal_ko, M. I. Katsnelson, U. Zeitler, D. Jiang, et al., "Unconventional quantum Hall effect and Berry's phase of 2π in bilayer graphene", Nature Physics, 2, 177, 2006.

[22] E. McCann, "Asymmetry gap in the electronic band structure of bilayer graphene", Physical Review B, 74, 161403, 2006.

[23] S. Y. Zhou, G.-H. Gweon, A. V. Fedorov, P. N. First, W. A. de Heer, D. -H. Lee, F. Guinea, et al., "Substrate-induced bandgap opening in epitaxial graphene", Nature Materials, 6, 770, 2007.

[24] J. Hass, F. Varchon, J. E. Mill´an-Otoya, M. Sprinkle, N. Sharma, W. A. de Heer, C. Berger, et al., "Why multilayer graphene on 4H-SiC(0001) behaves like a single sheet of graphene", Phys. Rev. Lett., 100, 125504, 2008.

[25] H. Lee, K. Paeng, I. Soo Kim, " A review of doping modulation in graphene", Synthetic Metals 244, 36–47, 2018.

[26] D. Wei, Y. Liu, Y. Wang, H. Zhang, L. Huang, G. Yu, "Synthesis of N-doped graphene by chemical vapor deposition and its electrical properties", Nano Lett. 9, 1752–1758, 2009.

[27] H. Liu, Y. Liu, D. Zhu, "Chemical doping of graphene", J. Mater. Chem. 21, 3335–3345, 2011.

[28] N. Peimyoo, J. Li, J. Shang, X. Shen, C. Qiu, L. Xie, W. Huang, T. Yu, "Photo controlled molecular structural transition and doping in graphene", ACS Nano 6, 8878–8886, 2018.

[29] C. Baekhap, L. Juno, L. Seungjun, K. Jae-Hyeon, L. Kyoung-Seok, O. Junghoon, H. Jongwoo, K. Yong-Hyun, C.I.S.P. Sungjin, "Generation of ultra-high-molecular-weight polyethylene from metallocenes immobilized onto n-doped graphene nanoplatelets", Macromol. Rapid Commun. 34, 533–538, 2013.

[30] Hakkim Vovusha,Suparna Sanyal, and Biplab Sanyal, " Interaction of Nucleobases and Aromatic Amino Acids with Graphene Oxide and Graphene Flakes", J. Phys. Chem. Lett. , 4, 21, 3710–3718, 2013.

[31] A. Hussain, S. Ullah, M. Arshad Farhan, "Fine tuning of band-gap of graphene by atomic and molecular doping: A density functional theory study", RSC Adv., 6, 55990, 2016.

[32] Ana S. Dobrota, Igor A. Pa˘sti, Slavko V. Mentus, B¨orje Johansson, Natalia V. Skorodumova, " Functionalized graphene for sodium battery applications: the DFT insights", Electrochimica Acta, Volume 250, 185-195, 2017

[33] Ali Shokuhi Rad, Sahand Sadeghi Shabestari, S. Mohseni a, S. A. Aghouzi, " Study on the adsorption properties of O_3, SO_2, and SO_3 on B-doped graphene using DFT calculations", Journal of Solid State Chemistry ,237, 204–210, 2016.

[34] Wu Qin, Xin Li, Wen-Wen Bian, Xiu-Juan Fan, Jing-Yao Qi, " Density functional theory calculations and molecular dynamics simulations of the adsorption of biomolecules on graphene surfaces", Biomaterials 31, 1007–1016, 2010.

[35] Lu CH, Yang HH, Zhu CL, Chen X, Chen GN, "A graphene platform for sensing Biomolecules", Angew Chem Int Ed Engl, 48(26), 4785–7, 2009.

[36] Yang X, Zhang X, Ma Y, Huang Y, Wang Y, Chen Y, "Superparamagnetic graphene oxide-Fe_3O_4 nanoparticles hybrid for controlled targeted drug carriers", J Mater Chem, 19,2710–4, 2009.

[37] Alwarappan S, Erdem A, Liu C, Li CZ. , " Probing the electrochemical properties of graphene nanosheets for biosensing applications", J Phys ChemC ;113, 8853–7, 2009.

[38] SamiraJafari, Hossein Derakhshankhah et al., "Mesoporous silica nanoparticles for therapeutic/diagnostic applications", Biomedicine & Pharmacotherapy, Volume 109, Pages 1100-1111,2019.

[39] A. Delmotte, E. W. Tate, S.N. Yaliraki and M. Barahona, "Protein multi-scale organization through graph partitioning and robustness analysis: application to the myosin-myosin light chain interaction", Phys Biol 8, 055010, 2011.

[40] N. Krishnamoorthy, M. H. Yacoub and S. N. Yaliraki, "A computational modeling approach for enhancing self-assembly and biofunctionalisation of collagen biomimetic peptides" Biomaterials, 32(30):7275-7285, 2011.

[41] R. J. Chen, S. Bangsaruntip, K. A. Drouvalakis, N. W. S. Kam, M. Shim, M. Y. Li, W Kim, P. J. Utz and H. Dai, "Noncovalent functionalization of carbon nanotubes for highly specific electronic biosensors", J. Proc. Natl. Acad. Sci. U.S.A. 100, 4984, 2003.

[42] R. J. Chen, Y. G. Zhang, D. W. Wang and H. J. J. Dai, "Noncovalent Sidewall Functionalization of Single-Walled Carbon Nanotubes for Protein Immobilization", J. Am. Chem. Soc. 123, 3838, 2001.

[43] Y. Kang, Y. C. Liu, Q. Wang, J. W. Shen, T. Wu and W. J. Guan, "On the spontaneous encapsulation of proteins in carbon nanotubes", Biomaterials 30, 2807, 2009.

[44] D. Pantarotto, C. D. Partidos, R. Graff, J. Hoebeke, J. P. Briand, M. Prato and A Bianco, "Synthesis, Structural Characterization, and Immunological Properties of Carbon Nanotubes Functionalized with Peptides ", J. Am. Chem. Soc. 125, 6160 , 2003.

[45] S. S. Wong, E. Joselevich, A. T. Woolley, C. L. Cheung and C. M. Lieber, "Covalently functionalized nanotubes as nanometre-sized probes in chemistry and biology", Nature 394, 52, 1998.

[46] Z. G. Chen, J. Zou, G. Liu, F. Li, Y. Wang, L. Z. Wang, X. L. Yuan, T. Sekiguchi, H. M. Cheng and G.Q. Lu, "Novel Boron Nitride Hollow Nanotubes", ACS Nano 2, 2183, 2008.

[47] G. Ciofani, "Potential applications of boron nitride nanotubes as drug delivery systems", Expert Opin. Drug Deliv 7, 889, 2010.

[48] S. Gowtham, R. H. Scheicher, R. Ahuja, R. Pandey and S. P. Karna, "Physisorption of nucleobases on graphene: Density-functional calculations ", Phys. Rev. B 76, 033401, 2007.

[49] A. Das, A. K. Sood, P. K. Maiti, M. Das, R. Varadarajan and C. N. R. Rao, "Binding of nucleobases with single-walled carbon nanotubes: Theory and experiment", Chemical Physics Letters 453, 266 , 2008.

[50] A. N. Enyashin, S. Gemming and G. Seifert, " DNA-wrapped Nanotubes", Nanotechnology 18, 245702, 2007.

[51] S. Gowtham, R. H. Scheicher, R. Pandey, S. P. Karna and R. Ahuja, "First-principles study of physisorption of nucleic acid bases on small-diameter carbon nanotubes", Nanotechnology 19, 125701, 2008.

[52] E. S. Jeng, A. E. Moll, A. C. Roy, J. B. Gastala and M. S. Strano, " Detection of DNA hybridisation using the near infrared band gap fluorescence of single-walled carbon nanotubes", Nano Letters 6, 371,2006.

[53] R. R. Johnson, A. T. C. Johnson and M. L. Klein, "Probing the Structure of DNA−Carbon Nanotube Hybrids with Molecular Dynamics ", Nano Letters 8, 69, 2008.

[54] S. Meng, P. Maragakis, C. Papaloukas and E. Kaxiras, "DNA Nucleoside Interaction and Identification with Carbon Nanotubes", Nano Letters 7, 45, 2007.

[55] F. Ortmann, W. G. Schmidt and F. Bechstedt, "Attracted by Long-Range Electron Correlation: Adenine on Graphite ", Phys. Rev. Lett. 95, 186101, 2005.

[56] X. M. Tu, S. Manohar, A. Jagota and M. Zheng, "DNA sequence motifs for structure-specific recognition and separation of carbon nanotubes", Nature 460, 250 , 2009.

[57] D. A. Heller, E. S. Jeng, T. K. Yeung, B. M. Martinez, A. E. Moll, J. B. Gastala and M. S. Strano, " Optical detection of DNA conformational polymorphism on single-walled carbon nanotubes ", Science 311, 508, 2006.

[58] A. Rajendran, C. J. Magesh and P. T. Perumal, Bba-Gen Subjects, "DNA-DNA cross-linking mediated by bifunctional [SalenAlIII]+ complex", 1780, 282, 2008.

[59] R. Hong, N. O. Fischer, A. Verma, C. M. Goodman, T. Emrick and V. M. Rotello, Control of Protein Structure and Function through Surface Recognition by Tailored Nanoparticle Scaffolds", J. Am.Chem. Soc 126, 739, 2004.

[60] C. C. You, S. S. Agasti, M. De, M. J. Knapp and V. M. Rotello, "Modulation of enzyme–substrate selectivity using tetraethylene glycol functionalized gold nanoparticles", J. Am. Chem. Soc 128, 14612, 2006.

[61] Y. Cui, Q. Q. Wei, H. K. Park and C. M. Lieber, "Nanowire nanosensors for highly sensitive and selective detection of biological and chemical species ", Science 293, 1289 , 2001.

[62] H. Benyamini, A. Shulman-Peleg, H. J. Wolfson, B. Belgorodsky, L. Fadeev and M. Gozin, " Interaction of c(60)-fullerene and carboxyfullerene with proteins: docking and binding site alignment", Bioconjugate Chemistry 17, 378, 2006.

[63] C. Staii and A. T. Johnson, "DNA-Decorated Carbon Nanotubes for Chemical Sensing", Nano Letters 5, 1774, 2005.

[64] P. Singla, M. Riyaz, S. Singhal and N. Goel, " Theoretical study of adsorption of amino acids on graphene and BN sheet in gas and aqueous phase with empirical DFT dispersion correction", Phys. Chem. Chem. Phys., 18, 5597, 2016.

[65] H. Luo, H. Li, Q. Fu, Y. Chu, X. Cao, C. Sun, X. Yuan and L. Liu, " Density functional theory study on the interactions of L-cysteine with graphene: adsorption stability and magnetism", Nanotechnology, 24(49), 495702, 2013.

[66] Shihai Zhang, Xiangfang Zeng, Man Ren, Xiangbing Mao and Shiyan Qiao, " Novel metabolic and physiological functions of branched chain amino acids: a review", Journal of Animal Science and Biotechnology 8,10, 2017.

[67] H. Tavassoli Larijani, M. Darvish Ganji and M. Jahanshahi, "Trends of amino acid adsorption onto graphene and graphene oxide surfaces: a dispersion corrected DFT study", RSC Adv., 5, 92843, 2015.

[68] Jian-Houng Chen1, Hsin-Tsung Chen, "Computational explanation for interaction between amino acid and nitrogen-containing graphene Theoretical Chemistry Accounts" 137, 176, 2018.

[69] Xi Chen, Pengfei Gao, Lei Guo, Shengli Zhang, "Graphdiyne as a promising material for detecting amino acids", Scientific Reports, 5, 16720, 2015.

[70] I K Petrushenko, A I Tsar'kova , N I Tikhonov and K B Petrushenko, "Valine adsorption on pristine and N-doped graphenes: DFT, AIM, and IGM study", Mater. Res. Express 6, 125061, 2019.

[71] Preeti Singla, Mohd Riyaz, Sonal Singhal and Neetu Goel, "Theoretical study of adsorption of amino acids on graphene and BN sheet in gas and aqueous phase with empirical DFT dispersion correction", Phys. Chem. Chem. Phys., 18, 5597, 2016.

[72] Duy Khanh Nguyen, Ngoc Thanh Thuy Tran, Yu-Huang Chiu, Godfrey Gumbs and Ming-Fa Lin, " Rich essential properties of Si-doped graphene", Scientific Reports, 10, 12051, 2020.

[73] Diego Corte´s-Arriagada, Sebastia´n Miranda-Rojas, Daniela E. Ortegac and Alejandro Toro-Labbe´, "Oxidized and Si-doped graphene: emerging adsorbents for removal of dioxane", Phys. Chem. Chem. Phys., 19, 17587, 2017.

[74] M. D. Esrafili, R. Nurazar and E. Vessally, "Application of Si-doped graphene as a metal-free catalyst for decomposition of formic acid: A theoretical study", Int. J. Quantum Chem., 115, 1153–1160, 2015.

[75] Ying Chen, Bo Gao, Jing-Xiang Zhao Fu et al., "Si-doped graphene: an ideal sensor for NO- or NO_2-detection and metal-free catalyst for N_2O-reduction", Journal of Molecular Modeling volume 18, 2043–2054, 2012.

[76] YananTang, Zhiyong Liu et al., "Theoretical study on the Si-doped graphene as an efficient metal-free catalyst for CO oxidation", Applied Surface Science Volume 308, 402-407, 2014.

[77] Sathish Kumar Mudedla, Kanagasabai Balamurugan, "Interaction of nucleobases with silicon doped and defective silicon doped graphene and optical properties", Phys. Chem. Chem. Phys., 18, 295, 2016.

[78] P. Hohenberg and W. Kohn, "Inhomogeneous Electron Gas", Phys. Rev. 136, B864, 1964.

[79] W. Kohn and L. J. Sham, "Self-Consistent Equations Including Exchange and Correlation Effects", Phys. Rev. 140, A1133, 1965.

[80] M. Born and K. Huang, "Dynamic Theory of Crystal Lattices. Oxford: OxfordUniversity Press", 1954.

[81] V. Z. Fock, Z., "Näherungsmethode zur Lösung des quantenmechanischen Mehrkörperproblems", Phys. 61, 126, 1930.

[82] E. Schrödinger, "An Undulatory Theory of the Mechanics of Atoms and Molecules", Phys. Rev. 28, 1049, 1926.

[83] M. Born and R. Oppenheimer, "Zur Quantentheorie der Molekeln", Annalen der Physik 389, 457, 1927.

[84] D. R. Hartree, "The Wave Mechanics of an Atom with a Non-Coulomb Central Field. Part I. Theory and Methods." Proc. Cambridge Phil. Soc. 29, 9,1928.

[85] J. C. Slater, "The Theory of Complex Spectra", Phys. Rev. 34, 1293,1929.

[86] L.H. Thomas, "The Calculation of Atomic Fields", Proc. Cambridge Phil. Soc. 23, 542, 1926.

[87] E. Fermi, "Eine statistische Methode zur Bestimmung einiger Eigenschaften des Atoms und ihre Anwendung auf die Theorie des periodischen Systems der Elemente", Z. Phys. 48, 73, 1928.

[88] Martin, "Electronic Structure: Basic Theory and Practical Methods, CambridgeUniversity Press, Cambrigde", 2004.

[89] Szabo and N. S. Ostlund, "Modern Quantum Chemistry: Introduction to AdvancedElectronic Structure Theory. McGraw-Hill, New York", 1989.

[90]. A. D. Becke, "Density-functional exchange-energy approximation with correct asymptotic behavior, Phys. Rev. A 38, 3098,1988.

[91] P. Perdew, K. Burke and M. Ernzerhof, "Generalized Gradient Approximation made simple", Phys. Rev. Lett. 77, 3865,1996.

[92] J. P. Perdew, K. Burke, and Y. Wang, "Generalized gradient approximation for the exchange-correlation hole of a many-electron system", Phys. Rev. B 54, 16533,1996.

[93] F. Giustino, "Materials Modelling using Density Functional Theory, Oxford UniversityPress, New York", 2014.

[94] P. Hobza, J. Sponer and T. Reschel, "Density functional theory and molecular clusters",J. Comput. Chem. 11, 1315,1995.

[95] M. Allen and D. J. Tozer, "Helium dimer dispersion forces and correlation potentials in density functional theory", J Chem. Phys. 117, 11113,2002.

[96] S. Baroni, P. Giannozzi and A. Testa, "Green-function's approach to linear response in solids" Phys. Rev. Lett. 58, 1861,1987.

[97] S. Kristyan and P. Pulay, "Can (semi)local density functional theory account for the London dispersion forces?", Chem. Phys. Lett. 229, 175, 1994.

[98] S. Grimme, "Semiempirical GGA-type density functional constructed with a long-range dispersion correction", J. Comput. Chem. 27, 1787,2006.

[99] P. Giannozzi, S. Baroni et al, "QUANTUM ESPRESSO: a modular and open-source software project for quantum simulations of materials", J.Phys.:Condens.Matter 21, 395502, 2009.

[100] Kim S, Chen J, Cheng J et al, "PubChem in 2021: new data content and improved web interfaces", Acids Res., 2021

[101] Rosa Di Felice,Annabella Selloni, and Elisa Molinari "DFT Study of Cysteine Adsorption on Au(111)", J. Phys. Chem. B, 107, 1151-1156, 2003.

[102] Basant Roondhe and Prafulla K. Jha "Haeckelite, a new low dimensional cousin of boron nitride for biosensing with ultra-fast recovery time: a first principles investigation", J. Mater. Chem. B, 6, 2018.